USING PRESCRIPTION MAPS FOR IN FIELD EVALUATION OF PARAMETERS AFFECTING SPRAYING ACCURACY OF A SELF-PROPELLED SPRAYER

A Thesis
Submitted to the Graduate Faculty
of the
North Dakota State University
of Agriculture and Applied Science

By

John Christopher Mayer

In Partial Fulfillment of the Requirements
for the Degree of
MASTER OF SCIENCE

Major Department:
Agricultural and Biosystems Engineering

November 2021

Fargo, North Dakota

North Dakota State University
Graduate School

Title

USING PRESCRIPTION MAPS FOR IN FIELD EVALUATION OF PARAMETERS AFFECTING SPRAYING ACCURACY OF A SELF-PROPELLED SPRAYER

By

John Christopher Mayer

The Supervisory Committee certifies that this ***disquisition*** complies with North Dakota State University's regulations and meets the accepted standards for the degree of

MASTER OF SCIENCE

SUPERVISORY COMMITTEE:

Dr. Paulo Flores
Chair

Dr. Thomas Bon

Dr. Michael Ostlie

Approved:

11/27/2021
Date

Dr. Kenneth Hellevang
Department Chair

ABSTRACT

Advanced sprayer control systems aim to improve accuracy and reduce waste in spray application. The objective of this study was to determine an optimum prescription map cell size/resolution that is compatible with current technology. A prescription map with several cell sizes was created and tested in field conditions to evaluate the effect different cell size parameters have on spray accuracy. The outcomes show that the dependent variable cell width had the greatest effect on application accuracy (p-values < 0.05), followed by cell length, and that an optimum cell width of 1.5 m [4.92 ft], a length of 3.05 m [10 ft], and application speed of 10.3 km h^{-1} [6.4 mph] is recommended. To further refine this analysis, the testing should be expanded with the inclusion of a variety of manufacturers and equipment and a test prescription map with a truly randomized cell distribution to better reflect actual field conditions.

ACKNOWLEDGMENTS

First and foremost, I would like to express my sincere thanks to my advisor, Dr. Paulo Flores, as he provided me with his expertise, guidance, and encouragement during my graduate study. Thank you for all the time and assistance you have afforded me along the way, it is greatly appreciated.

I would also like to thank my research committee members Dr. Thomas Bon and Dr. Michael Ostlie for the input and support that has guided me. I am grateful for the time taken to ensure my success.

I would like to thank the North Dakota State University Carrington Research Extension Center for the use of their facilities and equipment, especially for providing access to the Case Patriot 4440 sprayer.

A special thanks to all my family members and friends for their constant support and encouragement in my endeavors.

TABLE OF CONTENTS

LIST OF TABLES

LIST OF FIGURES

LIST OF APPENDIX TABLES

LIST OF APPENDIX FIGURES

1. INTRODUCTION

Weed presence continues to reemerge year over year, chemical costs continue to increase, and chemical usage continuing to face increasing government oversight, are just a few of the challenges that site-specific weed management intends to address by minimizing wasted application of chemicals and reducing environmental load of active ingredients. Thus, sprayer system manufacturers have developed precision spray systems that allow the individual spray nozzles to be controlled precisely. These spray systems are designed to reduce the waste of overspray, which helps to minimize costs while still providing adequate protection (CaseIH, 2020).

Weed pressure on crops influence the yield potential by competing with the crop for nutrients, sunlight, and moisture. To maximize crop yield, this weed pressure should be minimized by targeting and eliminating the weeds competing with the crop. For some crops like corn (*Zea mays* L.) and soybean (Glycine max L.), significant weed pressure has been shown to reduce yield by up to 35% (Gašparović, 2020).

Although several sprayer systems have been developed for more accurate control of spray application, not all systems are the same. Some spray systems are controlled in sections with large groups of multiple nozzles, while other systems can be controlled down to the individual nozzle. Three-section systems offer approximately an 8% reduction in application area and a five-section system offer approximately an 11% reduction (Luck et al, 2010). This shows that an increase in controllable sections results in an increase in application accuracy. It is unclear how much of a reduction individual nozzle control will provide, but it is likely greater yet.

To obtain accurate chemical application, precision spray systems with a high level of nozzle control can be utilized for weed management. There are several factors affecting herbicide application with the performance of the spray application system playing a determining role in the

final herbicide coverage (Luck et al, 2011). Compared to sprayer systems that have large sectional control, there are not many studies conducted on the resolution or minimum cell size required to utilize the full capability of the sprayer systems that offer individual nozzle control. An optimum cell size or resolution for the spray prescription map could help producers plan their site-specific weed management (SSWM) herbicide application while still guaranteeing coverage.

1.1. Objectives

The goal of this project is to determine an optimum cell size or resolution for a prescription herbicide application map, which guarantees acceptable coverage needed to eliminate the weeds identified by an unmanned aerial system (UAS) flight. A prescription map utilizing several cell sizes will be created and tested to determine the optimum cell size for a set of normal operating conditions. The major objectives of this project are as follow:

1. To determine an optimum prescription map cell size/resolution that is compatible with current technology.
    a. Determining an optimum cell width and cell length.
    b. Determining an optimum ground speed for accuracy.
2. Assess spray accuracy by comparing the prescription map to the as-applied map recorded by the sprayer system.

2. LITERATURE REVIEW

Precision farming techniques are being adopted by producers with the hopes of improving yields and profitability by reducing waste and other risks associated with farming. Precision farming centers around the premise that agronomic decisions are made based upon localized observations in a field, as a way of addressing field variability, reaching down to the level of a single plant (Cossette, 2019). Effective weed control is a crucial operation in crop production as inefficient weed management reduces yields and can lead to detrimental environmental impacts. A significant weed presence in fields is capable of causing a significant reduction in potential crop yield, with losses of up to 35% reported (Gašparović, 2020). There are several precision chemical application technologies in current use to help reduce the inefficient use of herbicide without also causing an increase in weed presence, however these technologies still have room for optimization.

When it comes to weed management, most producers uniformly spray herbicides across the field, a result of the lack of access to site-specific technology (Gerhards, 2006). Uniform application of herbicides across a field tends to lead to overapplication due to the predominant patchy weed distribution (Jurado-Expósito et al. 2003). An alternative approach is site-specific weed management (SSWM) that can help farmers reduce waste of chemical herbicides that are sprayed on the crop or soil by applying only in areas with the intended target, weeds (Christensen, 2009). SSWM recognizes that there is significant variability within a field, and therefore treatment needs to be adjusted to match that variability (Michaud et al., 2008).

Implementing SSWM on self-propelled sprayers requires specialized equipment, both hardware and software. This equipment comes at a premium cost and may not be compatible with all sprayer manufacturers. An example of this specialized equipment is the Raven Viper 4+ controller (Raven Industries, Sioux Falls, SD), which costs upwards of $9000 US (Mid-South,

2020). That cost doesn't include the additional paid software feature unlocks required for reading and applying prescription maps, nor the physical hardware on the sprayer boom. The AIM Command FLEX upgrade option for the Case IH self-propelled sprayers that adds the pulse-width modulation (PWM) capable nozzles and other hardware adds an additional $32000 to the price of the unit (CaseIH, 2020).

The sprayer is one critical component of implementing a SSWM spraying system, another is how the weed presence is assessed. At the time of this writing, the author was unaware of any sensor solution that would allow a commercial sprayer to implement SSWM by differentiating crop form weeds in the early growing season. Unmanned aerial systems (UASs) are a promising tool to accomplish that task, since they can be used to map weed distribution in a field. That map data then needs to be converted into a usable form that the sprayer control system can act upon. Possible advantages of implementing SSWM using UAS data include: 1) the sprayer can utilize the manufacturer's systems without requiring custom/aftermarket solutions; 2) the sprayer can operate at closer to normal spraying speeds since data processing is completed ahead the field spraying operation, unlike other real-time systems that complete the data processing while in the field. The challenge is creating and implementing a map that factory sprayer systems can utilize with an acceptable degree of accuracy.

2.1. Site Specific Weed Management

From a remote sensing perspective, there are two categories of weed mapping/identification, proximal (ground-based) and aerial (satellite- and airborne-based) sensing. Commonly, remote sensing for SSWM, utilizes a map-based approach of data collection, analysis, and identification for further use with several exceptions. In contrast, real-time systems simultaneously detect and control weeds (López-Granados, 2010). Examples of real-time spray

systems include those produced by Bosch, Trimble, and John Deere. The Trimble WeedSeeker 2 spray system utilizes sensor modules mounted ahead of each nozzle along the spray boom to detect weeds and trigger the nozzle to dispense herbicide (Trimble, 2019). It is important to note that these technologies have not been developed to the point of distinguishing between crop and weed, making it unsuitable to control only weeds during most of the growing season. The Bosch smart spray system speed is limited by the processing time required to analyze the image captured by the camera and the spray nozzle passing the weed, about 300 milliseconds (Bosch, 2020). It should be noted that this study is being conducted as part of a project that uses UAS imagery to discriminate between crops and weeds for creation of site-specific prescription maps.

Satellite imagery is a mature technology that continues to become more useful with resolution improvements. Although the resolution gap between satellite and airborne imagery has narrowed significantly with the availability of high-resolution sensors such as IKONOS, Sentinel-2, and QuickBird, satellite imagery still trails behind other airborne imagery systems regarding resolution (Yang et al., 2013). This does not negate the value that satellite imagery can provide as a useful source of mapping data when used for other precision agriculture applications. For the purpose of weed identification, satellites currently do not provide enough resolution to identify or map weeds growing in a crop field.

UASs provide benefit to producers through monitoring crop and soil, as well as field mapping. UASs are highly adaptable by design, capable of carrying a variety of payloads such as moisture, temperature, and chemical composition sensors (Fultz, 2018). The versatile nature of some of those aircrafts can also accommodate high-definition camera and image-recognition sensor packages that provide crop monitoring data (Kirkpatrick, 2019). Some of the cameras most commonly found on UASs are Red-Green-Blue (RGB), thermal, multispectral, and hyperspectral.

When the sensor package is properly configured, it is possible to collect all data types on a single pass. (Kirkpatrick, 2019).

An important parameter of remote sensing is the spatial resolution determined by the pixel size of the sensor unit. A suitable pixel size is determined by the smallest discernable feature and accuracy, while meeting the rough rule requiring four pixels to detect the smallest objects (Hengl, 2006). The sensor platform used for image collection has spatial resolution limitations built in because of current technological limitations. Generally, satellite imagery offers the poorest resolution with an approximate 2.7 m resolution and are therefore at a disadvantage. Satellite resolution is followed by manned aircraft with and approximate 1.87 m resolution, and UAV offering the highest resolution of approximately 0.15 m resolution (López-Granados, 2011). Today, the resolution of UAV systems continues to increase, and it is possible to easily achieve a resolution of between 1-5 cm (Torres- Sánchez et al., 2013). Higher resolutions are possible when flying much closer to the ground at the cost of limiting the area covered by each flight. This high spatial resolution adds to the generalization that UAS images are more feasible for use in weed mapping (Haung et al., 2020). The spatial resolution ultimately depends on the specific sensor setup used for data collection. While high-resolution imagery to map weed presence is critical, just as important to SSWM is precise auto-steering and nozzle control capabilities covered in the next section.

2.2. Current Auto-guidance Technologies in Use

Global positioning system (GPS) guidance is one of the most mature precision farming technologies currently in use. GPS signal was made available for civilian use in 1983 by the U.S. government. This new technology was adapted for agricultural use within 10 years of its release (Marsh, 2018). GPS guidance aids the operator in keeping a straight path which helps to reduce

overapplication or underapplication by avoiding overlap and skips, respectively, during application of agricultural products (Schimmelpfennig, 2016). Lightbar guidance systems are an example of guidance systems that utilize GPS but do not steer the tractor, providing only a visual indicator if the operator is off-line (Laws, 2004). Since the lightbar system relies on input from the operator to steer the equipment in the field, that system is deemed less accurate than auto-steer systems and it is not ideal for application with SSWM.

Automated steering, known as auto-steer, uses a GPS signal to direct the path of the machinery. This method requires no steering input from the operator while travelling up and down the field, for all intents and purposes, letting the machine drive itself (Hill, 2009). The operator is still required to manually make the turns at the ends of the field and follow the field edges. Auto-steer technology reduces overlap and skips by the machinery with greater positional accuracy than traditional GPS guidance. The greatest positional accuracies by machinery are seen with systems that incorporate integral valve systems with a real time kinematic (RTK) GPS receiver (Cossette, 2019). An example of that is the John Deere StarFire 6000 receiver. The base model offers horizontal pass accuracy of +/- 15 cm. When utilizing the RTK options a positional accuracy of +/- 2.5 cm, can be achieved along with a long-term repeatability of +/- 2.5 cm (Deere & Company, 2020). A higher positional accuracy lends well to optimal farming practices and helps magnify the beneficial elements of other guidance related technologies.

In addition to auto-steer capabilities, most modern sprayers, and upgraded legacy sprayers, have the capability to generate a coverage map that records where the sprayer had been and how much product was applied as it traveled over the field. These “as-applied” maps are traditionally used post application for reporting and analysis at the end of the season. The “as-

applied" maps are also used to trigger the nozzle or section control to spray any skipped areas that may result from the path chosen to cover the field (CaseIH, 2020).

2.3. Nozzle Control Technologies

Today most sprayers operate with selective section control that partitions the implement into smaller controlled sections with the herbicide dosage regulated by pressure in the hydraulic system and standard spray nozzles (Gerhards and Oebel, 2006). Around 70% of self-propelled sprayers currently used by producers in the Midwest region of the United States are equipped with automatic section control (ASC) (Hollis, 2011). ASC is used to reduce application of herbicide to unwanted areas such as overlap on field ends and edges by turning off the section that overlaps previously applied areas (Sharda et al., 2012). The boundaries of the application areas are determined by georeferenced coordinates generated by the GPS receiver (Luck et al., 2011). Studies conducted by the University of Kentucky showed that ASC can reduce chemical overlap waste by 2.3% to 14.5% with the reduction of overlap, depending on the number of control sections (Luck et al., 2011). However, ASC is not the only technology in current use to minimize herbicide application inefficiencies.

In conjunction with ASC, rate controllers have been adopted to maintain the application by controlling the flow of product. Rate control systems strive to maintain a targeted rate regardless of external factors, such as ground speed changes or boom width (Ayers et al., 1990). Width control resolution decreases as the number of control sections increases, however with an increase in the number of control sections there is an increase in processing requirements and response times for system actuation and speed changes (Sharda et al., 2012). Control system latency results in an inherent time delay that occurs when rate adjustments are required during operation. A control system response time of up to 2.2 seconds can be observed while utilizing a Differential Global

Positioning System (DGPS) receiver with a horizontal accuracy of 1 m (Al-Gaadi and Ayers, 1999).

Pulse width modulation (PWM) is one of the key technologies that allow a self-propelled sprayer to maintain a uniform volume across the boom regardless of external factors. PWM technology is one modulation method of electrical pulse signals. The method controls the output device by changing the duty cycle, where the duty cycle is the process of switching the supplied power on and off at a fast rate (Wei et al., 2011). Adjusting the duty cycle of the PWM signal changes the output power and the valve opening is controlled, realizing control of the spray flow (Wei et al., 2009). PWM adapted to spraying technology helps ensure constant application rate and pressure by varying the duty cycle as speed changes. When properly equipped, the PWM system currently utilized by Case IH on their self-propelled sprayers operates at 10 pulses per second and can maintain consistent rate and pressure with speed ranges of up to 8:1, or $1/8^{th}$ of rated full speed (CaseIH, 2020). Another benefit to PWM spray systems, is the capability of fast valve response times that result in no pressure bleed-down or nozzle dribble at turn-off (CaseIH, 2020).

Variable spray angle fan spray nozzle (VSAFSN) is a technology that strives to improve upon spray coverage inaccuracies resulting from vertical boom whip (Nalavade et al., 2008). Boom whip is especially prevalent in sprayers that utilizes long booms and is gaining importance as sprayer boom lengths continue to increase. VSAFSN controls the spray angle in relation to the boom to maintain desired ground spray footprint. As with PWM, time of response of the nozzles may limit the performance of VSAFSN when the system is traveling at a fast speed. A VSAFSN system proposed for usage with PWM showed promising spray uniformity improvements for long spray booms susceptible to oscillation and the results showed that VSAFSN may not be required

for every nozzle across the length of the boom, but only the areas that are disproportionately affected by oscillation, which are mainly the ends of the boom (Ghasemzadeh and Humburg, 2016).

2.4. Integration of UAS Imagery and Sprayer Technologies

Geographical Information Systems (GIS) are a visual tool generally for the purpose of simulation, analysis, and building models. GIS use for agriculture purposes started with several agricultural companies using simplified software to generate crop yield maps. There are numerous studies of GIS software being used for analysis and simulation (Michaud et al., 2008). In precision agriculture the emphasis is on mapping the variability across the field and acting upon that variability using treatments specific to each area. Because of this, GIS software plays a critical role implementation. GIS offers a good way to analyze and transfer the UAS imagery to a sprayer when used as a conduit between converting a weed map to a prescription map because of the need to match the position of various layers.

There are few reports in the literature that deal with the implementation of site-specific spray control management into full-sized self-propelled sprayers. One that was identified utilized custom-built software applications, written in C/C++, for translating weed map data from a GIS program into a spray coverage map that could be used to control the sprayer control systems. The custom program required the use of an extra computer to control the valves and did not interface with any existing manufacturer controls (Michaud, 2008). Industry has advanced since 2008 and many of the big manufacturers utilize as applied maps that are generated during operation in the field to trigger the factory installed ASC systems (CaseIH, 2020). Manufacturer's tout fast response times and accuracy in spray control so adapting SSWM to utilize these options offers another benefit to customers with these systems.

Numerous studies have investigated the generation of weed maps for later use towards conversion to a spray prescription map. The studies centered around the method used for image analysis and weed identification. Most of the imagery was collected by UASs and used high-resolution multi-spectral sensor packages. Machine learning was used to process the raw data collected by the sensors, to classify what the pixel represents, and stitch together a weed map (Kamilaris & Prenafeta-Boldu, 2018; Hong et al., 2012). There are several methods that can be used to accomplish the task of identifying sensor data and translating the imagery.

In the broadest term, object-based image analysis (OBIA) involves pixels first being grouped based on a common trait such as spectral similarity. When used for row crop weed-sensing purposes OBIA consists of three phases: 1) crop row classification, 2) determination of crop and weeds, and 3) weed map generation. Using this method, a weed coverage map with 86% overall accuracy has been created (Pena et al., 2013).

Fully convolutional networks (FCN) are algorithms that incorporate automatic feature learning. Automatic feature learning is implemented through a forward and backward process conducted in end-to-end mode (Huang et al., 2018). Time required for data processing is an important characteristic for efficiency of different processing methods. Two weed map generation workflows were also evaluated with the mosaicking-labeling workflow outperforming the labeling-mosaicking workflow 0.22% overall accuracy and more importantly by doing so 7.7 min faster at 24.8 min (Huang et al., 2018).

A recent study was conducted comparing OBIA methods to FCN methods. The results showed that the deep learning FCN method outperformed the OBIA approach in both efficiency and accuracy with an overall accuracy (OA) of 90.3% and a mean intersection over union (MIU)

of 80.2% all while processing a 1000 x 1000 pixel input image in 326.8 milliseconds (Huang et al., 2020). The results demonstrate that FCN has good potential for use in SSWM applications.

Several studies go into detail on the hardware requirements needed to implement a SSWM system on a self-propelled sprayer (Christensen et al., 2009; Hong et al., 2012; Rasmussen et al., 2020). At a minimum, several key components are needed. First, a data collection method with UAS offering the best performance in this area for the reasons listed above. Second, a method of converting data into a prescription map in a timely manner with this accomplished mainly through the usage of high-performance computers and specialized software or customized algorithms (Haung et al.,2018). Third, the sprayer must have the capability of individual nozzle control or, less ideal, a high number of controllable sections. The sections should be of equal size to simplify the process of creating the prescription map. These nozzle or sections are controlled through the usage of electromechanical valves and controller interfaced with a precision guidance unit (Michaud, 2008). Fourth, there must be an interface that allows the controller to read/load the SSWM application map. This is where there is a deficiency in the current research with a lack of extensive testing on the limits of the current technology's capabilities.

3. MATERIALS AND METHODS

3.1. Background Information

Precision agriculture researchers at NDSU (Dr. Flores' research lab) have been working to develop a SSWM approach to control weeds in a corn field during the second herbicide application, when corn vegetative stage is between V4-V6. The approach consists of using UAS imagery to map the weeds in the corn field and use that map as the basis to create an herbicide prescription map. Once the weeds are mapped, a grid cell is overlaid on top of it, and a computer software is used to identify grid cells that have at least one weed within its boundaries. Cell with at least one weed in it are then selected to be sprayed, while the ones with no weeds present are not sprayed.

Since the conception of this approach for SSWM, in 2018, Dr. Flores had in mind to use a 3.1 x 3.1 m (10 x 10 ft) cell size, but due to hardware issues with the sprayer, the full field implementation of the approach was not possible in 2018. That first year, researchers were able to implement the SSWM approach using a 6.1 x 9.1 m (20 x 30 ft) (length x width) cell grid. That led to a reduction of 16% on acreage receiving an herbicide application. Further calculations demonstrated using the same weed data layer and by decreasing the grid cell size to 3.1 x 3.1 m (10 x 10 ft) or to 1 x 1 m (3.3 x 3.3 ft), the area not sprayed would go up to 40% and 70%, respectively.

Fast forward to 2021, Dr. Flores' research team was able to implement the whole approach from data collection to field spraying using a commercial size sprayer. Due to high density of weeds in the 2021 growing season, the cell size was decreased from a 3.1 x 3.1 m (10 x 10 ft) to a 0.5 m (1.6 ft) (single nozzle spacing) x 3.1 m (10 ft). That change was needed to justify the use of the SSWM, since a 3.1 x 3.1 m (10 x 10 ft) cell size would result in spraying over 95% of the field. Case IH engineers recommended that the application should stay below 11.3 km h^{-1} (7 mph), which

is the speed that would allow the sprayer with 10 Hz GPS receiver to resolve a distance 0.3 m (1 ft) per $1/10^{th}$ of second, or 3.1 m (10 ft) per seconds. With that in mind, researchers decided on an application speed of 10.5 km h^{-1} (6.5 mph), so the system was not constantly pushed to its limit.

With that background information in mind, the studies reported on this document aim to address questions regarding how cell dimensions (width and length) changes and application speed affect herbicide placement accuracy within the area of interest (within the cell).

3.2. Design Configuration of the Prescription Maps

To determine the optimum cell size for use in site specific weed management (SSWM) practices, several cell sizes should be tested at a variety of common spraying speeds. Existing OEM technologies allow for sectional control across the boom and upgraded controllers unlock the ability to further divide those sections to individual nozzle control. By leveraging those features, in addition to an RTK GPS receiver on the sprayer, and drone imagery with RTK accuracy, a study was designed to determine the impact of cell size width and length, and sprayer speed on the application accuracy based on a prescription map.

The study took place at the NDSU Carrington Research Extension Center (CREC, Carrington, ND). The area selected for the study was a relatively flat rye stubble field, which had been recently planted to millet.

The test site was mapped using a Phantom 4 RTK (DJI, Shenzhen, China) to collect georeferenced imagery with high spatial accuracy (+/- 2.5 cm [+/- 1 in]) (Figure 1), which would later be used as the background for creating the prescription maps used to apply the treatments for the study. The flight was at 76 m (249 ft) with a 75% overlap pattern. The Phantom 4 RTK utilizes a 2.5 cm (1 in), 20-megapixel CMOS sensor for image collection. Prior to the UAS flight, three 20 cm (8 in) orange pail lids were placed on the ground in a straight line (East-West direction) and

were secured with a 15 cm (6 in) nail (Figure 2). To help with locating the center of the lid from the UAS imagery, a black 5 cm (2 in) flat washer was inserted between the lid top and the nail head. The lids served as a reference corner for the computer-generated prescription maps (Southeast corner) and a ground reference (South edge) for the end of the sprayer boom.

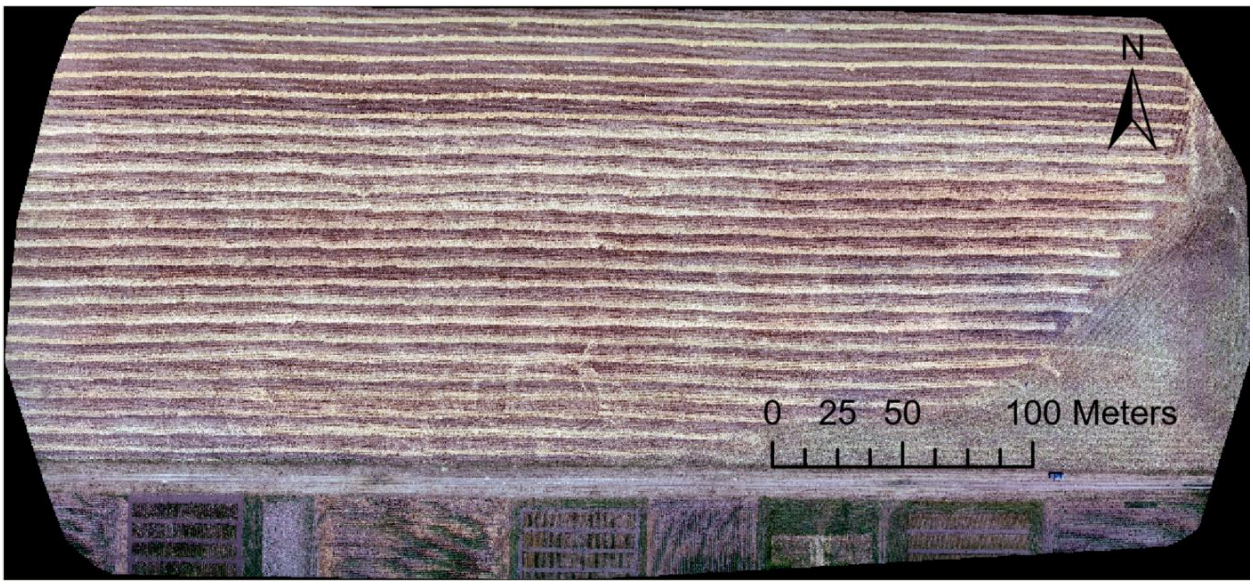

Figure 1. Aerial imagery from the study area used as the base to georeference the prescription maps to known ground point. Imagery collected by a DJI Phantom 4 RTK at 76 m [249 ft] AGL at the Carrington Research Extension Center, Carrington, ND.

Figure 2. Detail of the UAS imagery from the study location showing the known ground control point used to georeference the prescription maps. Orange plastic lid used as reference for the southeast corner of prescription map and south edge of sprayer boom. Imagery collected by a DJI Phantom 4 RTK at 76 m [249 ft] AGL at the Carrington Research Extension Center, Carrington, ND.

To test optimal cell size, a total of 150 individual cells were created. The width treatments chosen for testing were based on the original idea for the cell size 3 m (10 ft) wide, the cell size used on the corn study in the 2021 season 0.5 m (1.64 ft) wide, and an intermediate value 1.5 m (4.9 ft) wide. The length treatments chosen for testing were determined on both the nozzle cycle and GPS receiver refresh rate (10 Hz) and referencing the chosen application speeds and the distance that would be covered in the time the nozzles turn on/off. The speed treatments chosen for this study were based on the speed described on the spraying of a corn trial mentioned on item 3.1. Although the target speed on that study was 10.5 km h^{-1} (6.5 mph), the application speed was 10.3 km h^{-1} (6.4 mph). On this project, the intent was to test speeds that would allow one to cover acres per hour 13.5 km h^{-1} (8.4 mph) and a speed that would likely improve the herbicide placement accuracy 7.1 km h^{-1} (4.4 mph) by allowing more time for the controller to turn nozzles on and off. Table 1 shows more detailed information regarding the cell dimensions used on this research.

Table 1. Cell treatment dimensions (width x length) used in field studies to test the influence of cell width and length on herbicide placement accuracy. Based on a prescription map using a Case IH Patriot 4440 sprayer equipped with single nozzle control system.

Cell Size Identification	Cell Dimensions (m) [ft]	Area (m^2) [ft^2]	Number of Cells
SW (Small Width)	0.5x3.05 [1.64x10]	1.524 [16.4]	30
MW (Medium Width)	1.5x3.05 [4.92x10]	4.572 [49.2]	30
LW (Large Width)	3x3.05 [9.84x10]	9.144 [98.4]	30
SL (Small Length)	7.5x1.52 [24.61x5]	11.43 [123.0]	15
ML (Medium Length)	7.5x3.05 [24.61x10]	22.86 [246.1]	15
LL (Large Length)	7.5x4.57 [24.61x15]	34.29 [369.1]	15
XL (X-large Length)	7.5x6.10 [24.61x20]	45.72 [492.1]	15

The prescription maps start out as shapefiles created in ArcGIS Pro (ESRI, West Redlands, CA, USA). A 365 m (1,200 ft) long by 41.6 m (136.6 ft) wide rectangle was placed on the study area, with its southeast corner coinciding with the center of the most eastward pail lid from the UAS imagery. The rectangle was then subdivided into 0.5 x 1.52 m (1.64 x 5 ft) polygons that were then used to create the different cell sizes. Some of the treatments required some of those polygons to be combined into one (East-West) or both directions (East-West and North-South). An attribute field column was added to the shapefile's attribute table and the application rate of 56.8 l/ac (15 gal/ac) was assigned to that field. To accommodate the treatment speeds, it was necessary to create two shapefiles (Figure 3 and 4). That approach allowed for providing space between the first and third application for study and to change and stabilize sprayer speed. The cell treatments were organized on the prescription maps to create a randomized complete block design. The first prescription map file was used for the cell width trials, and the length and speed trials conducted at 10.3 km h^{-1} (6.4 mph) and 7.1 km h^{-1} (4.4 mph). The second prescription map file was used for the final length and speed trial conducted at 13.5 km h^{-1} (8.4 mph). That information is summarized in Table 2. It is easier and more controllable for the self-propelled sprayer to slow

from a faster speed than to speed up from a slower speed. The study required only two prescription maps to facilitate the three trials by creating the prescription maps in this manner.

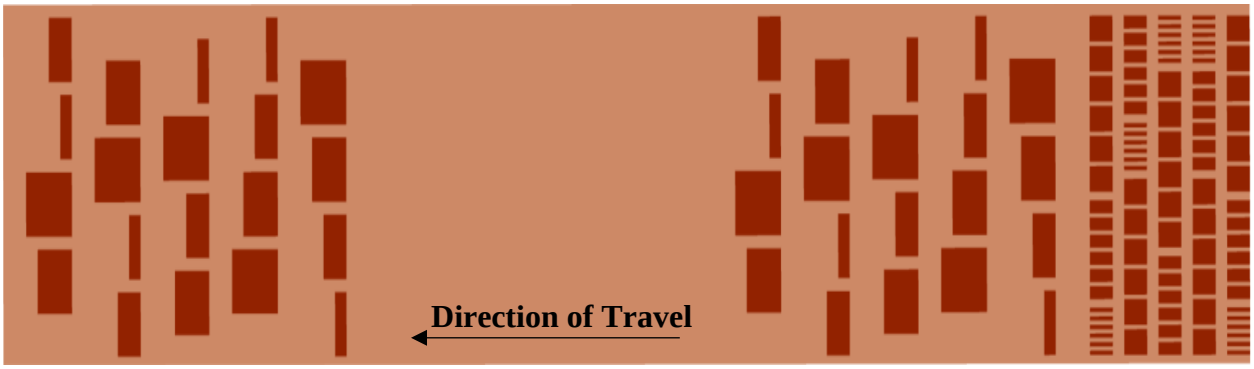

Figure 3. Prescription map generated by ArcGIS for AgLeader SMS for pass 1. From East to West, cell width study (3 treatments and 5 replications), and cell length study (4 treatments and 5 replications) at two speeds (10.3 and 7.1 km h^{-1}). Light color =0 gal/ac and dark color =15 gal/ac.

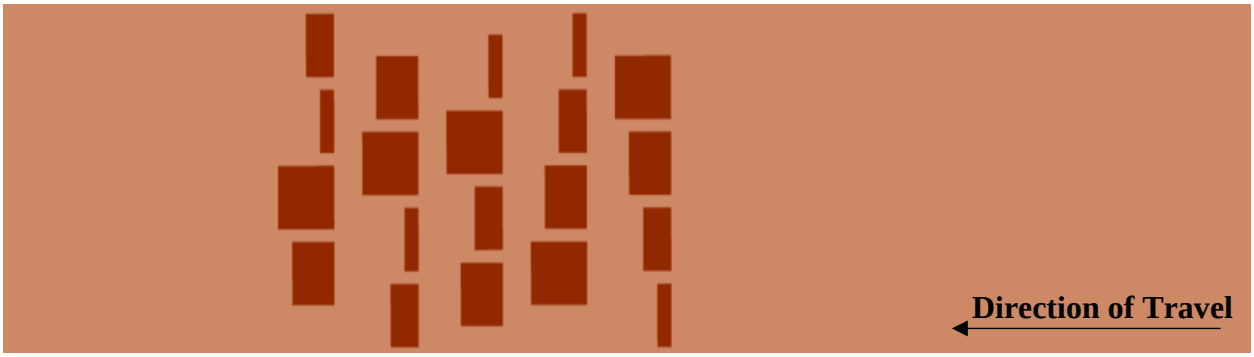

Figure 4. Prescription map generated by ArcGIS for AgLeader SMS for pass 2. Showing the length study (4 treatments and 5 replications) at the speed of 13.5 km h^{-1}. Light color =0 gal/ac and dark color =15 gal/ac.

Table 2. Application speed treatments used in field studies to test the influence of ground speed on herbicide placement accuracy. Based on a prescription map using a Case IH Patriot 4440 sprayer equipped with single nozzle control system.

Speed ID	Pass Used	Application Speed (km h^{-1}) [mph]
1	1	7.1 [4.4]
2	1	10.3 [6.4]
3	2	13.5 [8.4]

Treatments were separated by tested parameter. For the cell width study, variable width and constant length, an experimental unit consisted of six nozzles or sets of nozzles for each of the three cell widths (SW, MW, and LW; Table 1) across the boom. The experimental units were then randomized across the boom for each of the 5 replications of the study (Figure 5). The second study was designed to determine the effect of speed (7.1, 10.3, and 13.5 km h^{-1}; main plot) on the spraying accuracy of the dye solution using cells (sub-plots) with predetermined lengths (SL, ML, LL, and XL; Table 1) orientated parallel to the sprayer travel direction. The subplots were randomized across the boom for each of the 5 replications across the boom, and the cell widths were kept constant (7.5 m [24.6 ft] wide) (Figure 6). A detailed view of one of the speed treatment blocks is shown on Figure 7.

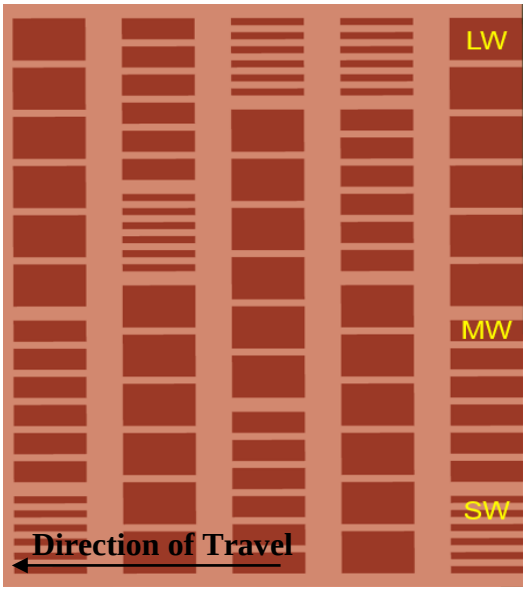

Figure 5. Detailed view of the field study to test the influence of cell width on herbicide placement accuracy. Based on a prescription map using a Case IH Patriot 4440 sprayer equipped single nozzle control system and travelling at 10.3 km h^{-1} (6.4 mph). 3 width treatments and 5 replications. Dark color =15 gal/ac, and light color =0 gal/ac.

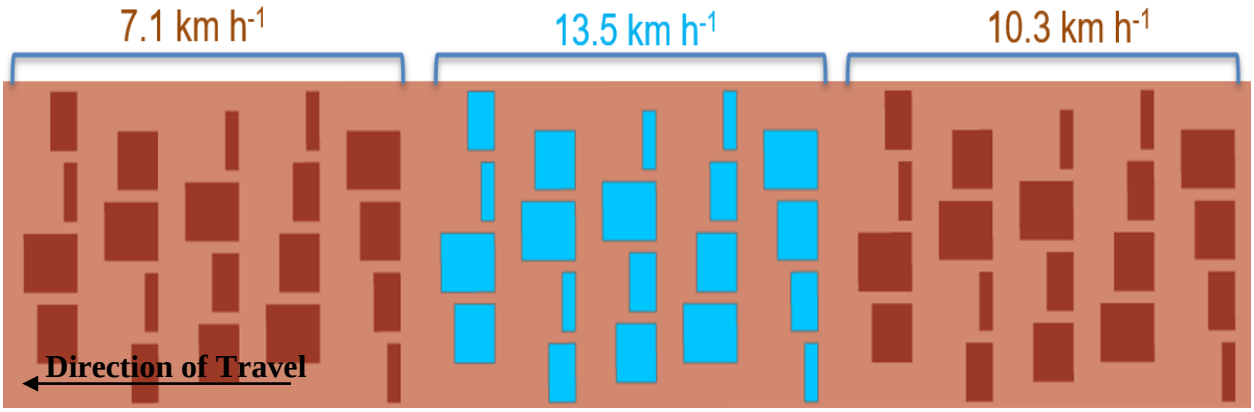

Figure 6. Detailed view of the main plot of the field study to test the influence of application speed on herbicide placement accuracy. Based on a prescription map using a Case IH Patriot 4440 sprayer equipped single nozzle control system. 3 speed treatments with 5 replications. Dark and blue colors =15 gal/ac, and light color =0 gal/ac.

Figure 7. Detailed view of the length sub-plots of the field study to test the influence of cell length on herbicide placement accuracy. Based on a prescription map using a Case IH Patriot 4440 sprayer equipped single nozzle control system and travelling at 10.3 km h^{-1} (6.4 mph). 4 width treatments with 5 replications. Dark color =15 gal/ac, and light color =0 gal/ac.

Once the shapefiles were edited to their final versions on ArcGIS Pro, those were imported into AgLeader SMS software (AgLeader, Ames, IA, USA) as prescription maps and exported to a Raven Viper Pro sprayer controller. That operation created the folder structure required by the Viper 4+ cab computer to run the prescription map created in AgLeader SMS.

With the intent to evaluate application accuracy by comparing UAS imagery to the prescription map, a visible dye was needed to identify the application areas. VISION PINK Fluorescent Dye Concentrate (Garrco Products, Converse, IN, USA) was selected for use as the visual indicator in conjunction with an anionic surfactant CONTROL DUO (Garrco Products, Converse, IN, USA). The sprayer was loaded with 852 L (225 gal) of water, 9.5 L [10 qts] of surfactant, and approximately 4.75 L (5 qts) of dye. This resulted in a medium rate of surfactant of 1.1 L per 100 L water (4.4 qts per 100 gal) and a double high rate of dye of 0.531 L per 100 L water (68 oz per 100 gal).

There was a period of 3-4 weeks between the first flight and the application of treatment. By that time, the millet was approximately 10.1-15.2 cm (4-6 in) tall (Figure 5).

Figure 8. A picture from the field test on the first day running the trials at the Carrington Research Extension Center (Carrington, ND). Millet height was around 10-15 cm (4-6 in). Flag indicates the location of the Southeast most orange pail lid and served to align the sprayer with the edge of the prescription map on the field.

3.3. Field Tests

Field testing was conducted to evaluate the performance of different cell widths and lengths at several application speeds. Prior to the initial test the sprayer boom was primed with treatment on another part of the field, taking approximately 208 L (55 gal) to ensure all nozzles were applicating the dye solution.

A CaseIH Patriot 4440 (Case IH, Racine, WI, USA) sprayer outfitted with a 41.6 m (136.6 ft) boom and equipped with Raven Viper 4 Plus cab controller (Raven Industries, Sioux Falls, SD, USA) running system version 21.1.0.51 was used to perform the test. An AFS 372 (Case IH, Racine, WI, USA) receiver provided the GPS link with a refresh rate of 10 Hz. The boom had 82 nozzles installed on a 0.51 m (20 in) spacing. The sprayer was equipped with Autoboom XRT that automatically controls boom height at 0.51 m (20 in). Combo-Jet SR110-08 (Wilger Industries, Saskatoon, Canada) small drop flat fan nozzle bodies were used during the dye application. Raven Hawkeye nozzles and three Raven Precision Boom Valves (Raven Industries, Sioux Falls, SD, USA) made up the individual nozzle control system. The nozzle control system installed on the sprayer had a cycle rate of 10 Hz. An image of the sprayer utilized for the field tests is shown in the appendix (Figure A1).

3.3.1. Initial Test

The initial test was carried out on 24 August, 2021. The meteorological conditions at the time of the initial trial were as follows: temperature of 21.6 °C (71 °F), air humidity 70%, dew point of 16.1 °C (61 °F), sky partly cloudy, and wind from the East at 11.3 km h^{-1} (7 mph). These conditions were conducive towards a good day for both spraying and image collection.

The prescription maps were loaded to sprayer using a USB stick. Once the maps were loaded, it took just a few minutes to conclude the application. Once the application was done, the as-applied maps were downloaded from the Viper 4+ for further analysis. An image of dye solution

being applied from the sprayer during the test is shown in the appendix (Figure A2). Two UASs were used to collect imagery data from the trials, the first was a DJI Phantom 4 RTK and the second was a DJI Matrice 200 series (DJI, Shenzhen, China) with a MicaSense Dual multispectral camera system (MicaSense, Seattle, WA, USA). The UAS flights were conducted at

Immediately after the applications it was noticed that the dye product applied did not perform as expected. There was no noticeable red color over the areas sprayed, which deemed the plans to use the drone imagery to assess spraying accuracy ineffective. A quick check of the images from the different drones flown immediately after the trial revealed similar results seen in the field, no red color over the sprayed areas (Figure 9).

Figure 9. Aerial image from the experimental area collected with a DJI Phantom 4 RTK at 30 m [100 ft] AGL immediately after application of red dye solution showing no indication of the dye application. Dye applied based on a prescription map and using a Case IH Patriot 4440 sprayer equipped single nozzle control system.

Another issue was found when comparing the as applied maps with the shapefiles created in ArcGIS. A noticeable difference between the two maps was observed. After some investigation, it was found that the SMS software was the culprit for the differences. For some reason, when the shapefiles were exported from SMS Advanced using the option “Export Full Device Setup to a Field Display/Monitor”, it modified the input file by blending some of the cells together and some

of the cells with the rate set for outside of the prescription area (0 gal/ac). The differences between the two maps are shown in Figure 10.

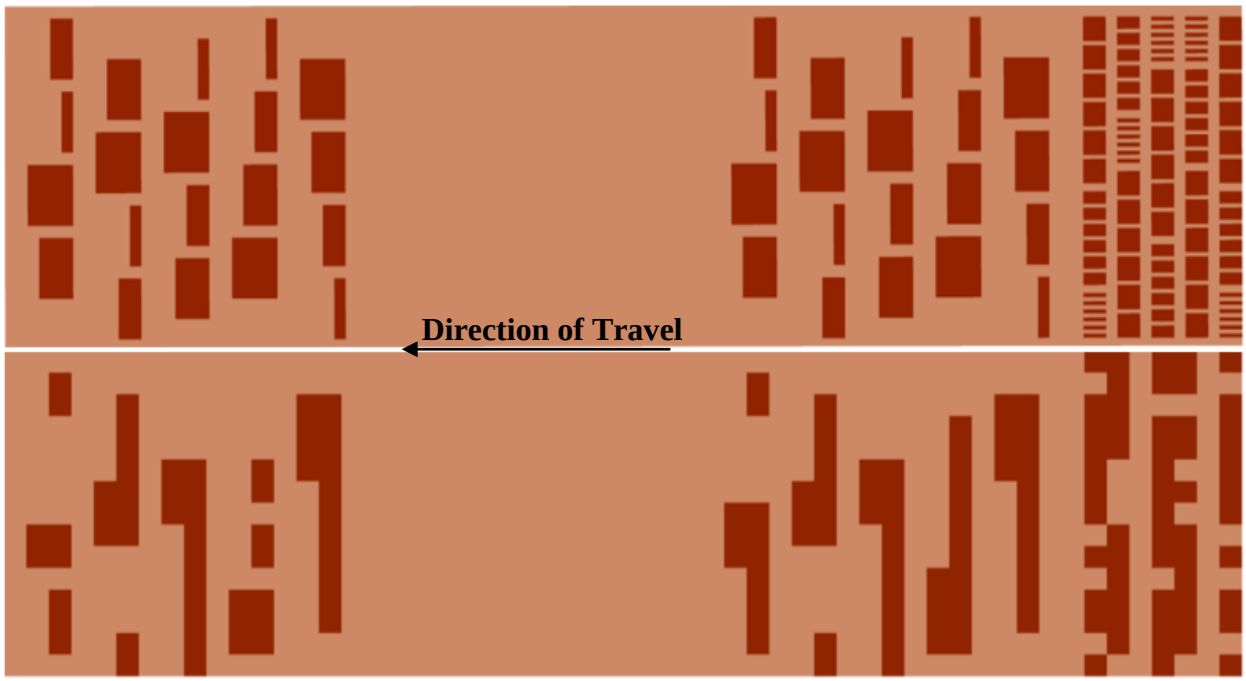

Figure 10. Target prescription map (top) and the prescription map exported from AgSMS software (bottom) showing the unwanted changes made by that software, resulting in a very different pattern than the one originally intended. Light color = 0 gal/ac, and dark color = 15 gal/ac.

3.3.2. Final Test

After some further investigation into the SMS Advanced issue during the prescription map export process, it was found that exporting the file using the option “Export to a Generic Format” yielded a prescription map as it was first generated in ArcGIS Pro. The next step was to use the folder structure previously created and substitute the prescription map files with the new one.

The second field test was carried out one day after the first one (25 August, 2021) with the same solution used for the first test, which had been kept on the sprayer. The same self-propelled sprayer as the initial test was used for the final testing and similar meteorological conditions were present at the time of the second test. Given the weather conditions, the availability of the sprayer

operator, and the lack of color produced by the dye solution in the sprayer, no drone imagery was collected from the field at the conclusion of the second test. Immediately after the test was concluded, the as-applied maps were downloaded from the Viper 4+ for further analysis. Comparisons for both the initial test and the final test are being made between the prescription map and the as-applied map.

3.3.3. Statistical Analysis

To analyze the test results for the varying cell width, a one-way ANOVA test was conducted in Microsoft Excel software (Microsoft, Redmond, WA, USA) as a randomized block design having three intended cell width treatments and five replications. Further statistical analysis was completed using SAS statistical software (version 9.4, SAS Institute Inc., Cary, NC, USA) as a randomized complete block design having four intended area size treatments, five replications, and was combined over three rates of travel treatments. For proportion variables, models assuming a gaussian distribution with identity linkage were compared with those of beta distribution and logit linkage using proc glimmix. Based on visible assessment of quartile-quartile plots of model residuals it was determined that data was best fit assuming a gaussian distribution with identity linkage (Figures A6 and A7). Formal analysis of all variables was thus completed using proc mixed under the assumption of normality. Significance was established at $\alpha = 0.05$. In instances where significant interaction was identified between rate of travel and intended area of application, tests of simple effects were used to assess variance within rate of travel treatments among intended area of application treatments. In all cases, treatment differences were tested using f-protected pairwise t-tests with a threshold of significance at $\alpha = 0.05$.

Due to having multiple replications for each test treatment, optimized treatments were determined by considering the lowest means of overspray and underspray percentage areas. Low

means of overspray and underspray percentage areas translate to high spray placement accuracy. So, there was only one optimized cell width, cell length, and application speed.

To keep the area of interest (AOI) standardized for all cell sizes, an additional width of 0.25 m on each side of the cells and an additional length of 0.75 m in front and behind each edge of the cells was determined to be the maximum area of evaluation. These AOI dimensions were chosen because the individual cells were spaced 0.5 m apart sideways (North-South direction) and spaced 1.5 m apart lengthwise (East-West direction). This resulted in an additional 0.5 m of width and an additional 1.5 m of length. Table 3 below shows the maximum outside areas for the cell testing.

Table 3. Summary of maximum allowable overspray areas used for analysis on the field studies testing the influence of cell width, cell length, and application speed on herbicide placement accuracy. Based on a prescription map using a Case IH Patriot 4440 sprayer equipped single nozzle control system.

Tested Parameter	Cell Size Identification	Maximum Overspray Area (m^2)
Width	SW (Small Width)	3.024
	MW (Medium Width)	4.524
	LW (Large Width)	6.774
Length	SL (Small Length)	12.762
	ML (Medium Length)	13.524
	LL (Large Length)	14.286
	XL (X-large Length)	15.048

Using ArcGIS, the prescription maps and the as-applied maps were intersected and merged using those respective ArcGIS tools. The as-applied polygons outside the target cell boundaries (overspray) were measured using the ArcGIS area measurement tool and compared against the maximum allowable values. The measured area was then divided by the target area of the cell interested in resulting in the overspray percent coverage area. The same process was conducted with the as-applied polygons within the target cell boundary with the addition of the resulting coverage percent area being subtracted from 100%. The leftover is the underspray

percent coverage area. Converting to overspray and underspray percent coverage areas allowed for a standard comparison between cell parameters irrespective of the change in target area that the changing parameters cause.

4. RESULTS AND DISCUSSION

4.1. Initial Test Cell Size and Application Speed Evaluation

As previously mentioned, the red dye used on the first trial of the study did not perform as anticipated. There was an expectation that after the solution application, the red dye would indicate where the solution was applied and that pattern would match the prescription map, which in turn would allow for accuracy to be assessed using UAS imagery using GIS software. Shortly after application, a field inspection showed that it was very difficult to find any trace of the dye in field. At that point, the only hope for analysis by this method was that the dye would show up on the multispectral imagery collected with the MicaSense Dual System that utilizes 10 multispectral bands, but no indication of the dye application was found on those images.

The backup plan to overcome the poor dye performance was to use the prescription map and superimpose it over the as-applied map to assess the spraying accuracy based on the target application area (prescription map) and the field applied area (as-applied map) (Figures A3 to A5). The as-applied map was retrieved from the Viper 4+ in-cab computer shortly after each trial of the study was completed. Due to some combination of operator and/or software issue, an as-applied map was created only from the first pass of the sprayer. At the same time, the research team realized that the as-applied map retrieved from the cab computer was very different from the intended prescription map (Figure 6).

Further investigation into the discrepancy revealed that the issue was due to internal settings pre-programmed into the SMS Advanced software that applied changes to the prescription map during the export process. These settings and changes are intended to make automatic adjustments to the prescription maps “to make it easier” on the equipment’s rate controller. Such

software adjustments are likely not an issue for large field operations but resulted in unforeseen problems for this study.

Another unforeseen problem that was initially encountered during the study was the Viper 4+ cab computer not reading the prescription map. It was diagnosed that the problem was caused by not having the feature "single product variable rate" unlock activated within the software. Raven was contacted and a 20-hour trial feature activation was provided, which allowed the sprayer to carry out the first test and again the next day for the second test.

As mentioned above, one as-applied map (first pass) was downloaded from the cab computer and evaluated to try to salvage some data from the initial testing. The results from the comparison between the software adjusted prescription map and the recovered as-applied map are shown in Table 4, which are the average values of spray accuracy by speed. Table 5 shows the results of the initial test broken down by target area, which shows that replications varied from 1 to 7 for each target area.

Table 4. Average underspray/overspray percent area values and number of replications for 2 application speeds. Collected from initial field trial using a Case IH Patriot 4440 and a prescription map with software varied target areas.

Speed ($km\ h^{-1}$) [mph]	# of Replications	% Area Undersprayed	% Area Oversprayed
10.3 [6.4]	17	28.16	22.08
7.1 [4.4]	10	5.97	31.13

Table 5. Initial field trial evaluation of spraying accuracy using a Case IH Patriot 4440 and a prescription map with software varied target areas. Cell parameters were varied and the results averaged across application speeds 10.3 km h^{-1} and 7.1 km h^{-1}.

Target Area (m^2)	# of Replications	Actual Coverage Area (m^2)	% Undersprayed	Overspray Coverage Area (m^2)	% Oversprayed
8	4	4.30	46.31	2.20	27.47
16	7	13.79	13.81	6.09	38.04
24	1	19.73	17.79	8.79	36.63
32	2	23.62	26.19	7.52	23.50
48	2	40.40	15.84	5.61	11.68
72	1	72.00	0.00	21.99	30.54
80	3	74.34	7.08	17.15	21.43
96	1	84.00	12.51	17.88	18.62
104	2	103.59	0.41	18.82	18.09
120	3	83.39	30.51	13.01	10.84
160	1	159.32	0.43	34.03	21.27

Analysis showed there were not enough replications of speeds tested to make any valid conclusions on effects of speed on spraying accuracy. However, the results also show that there is a statistically significant difference for both overspray and underspray with relationship to targeted cell size area (Figures 11 and 12). It means that, both overspray and underspray percentages had dependency on targeted cell area.

Although this initial trial had no defined cell widths and lengths controlled in an experimental manner, it does provide insight into how total targeted cell area affects the accuracy of the spray placement. It also shows a good baseline of how application speed affects accuracy. Slower application speeds reduce underspray, likely as a result of less ground being covered in the time that the GPS receiver refreshes position, and the nozzles turn on/off.

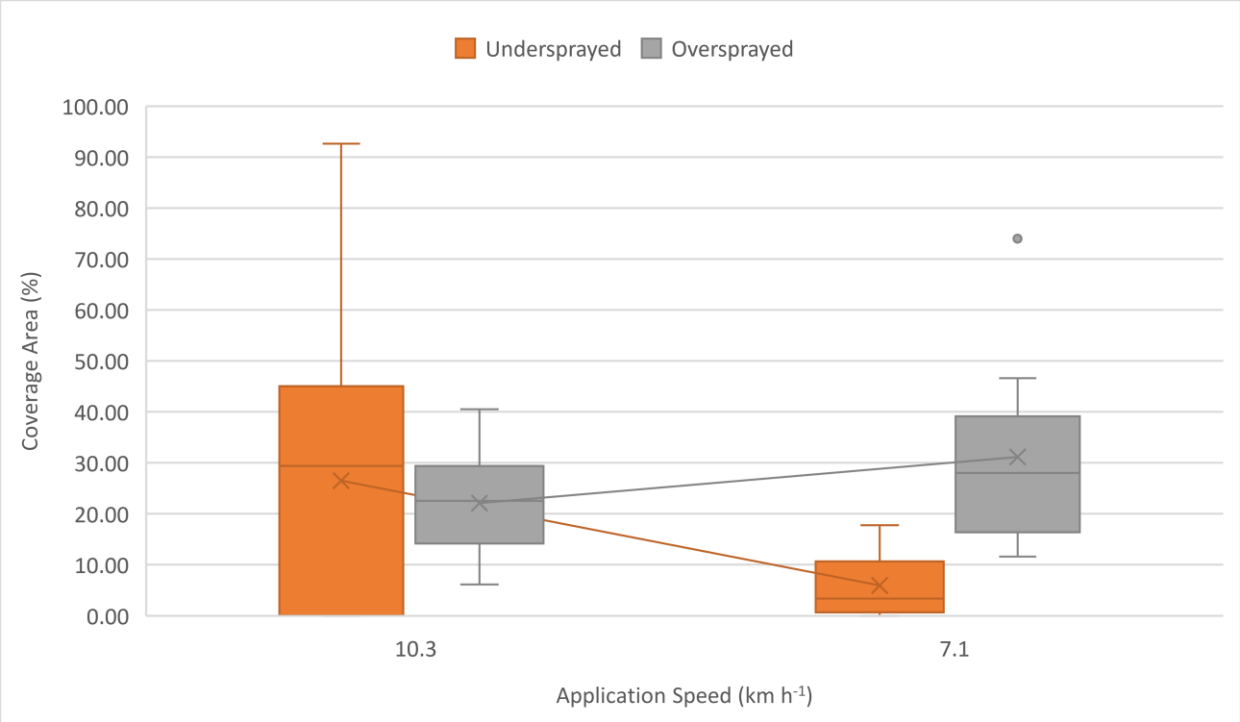

Figure 11. Spray coverage area accuracy percentage by speed for field trial 1. Conducted using a Case IH Patriot 4440 and a prescription map applicated at two speeds. Each box presents the distribution of coverage area percentage values for 17 replications for 10.3 km h^{-1} and 10 replications for 7.1 km h^{-1}.

According to Table 4 and Figure 10, overspray percent coverage areas decreased by 9.1% and undersprayed percentage coverage areas increased by 22.2%, which occurred at 7.1 to 10.3 km h^{-1} [4.4 to 6.4 mph]. The percentage underspray displayed a decreasing trend with a decrease in speed and percentage overspray trended towards increasing, but in no case was this significant.

The decrease in overspray percent coverage at a slower application speed is likely a result of less ground being covered during the system refresh time. The increase in underspray coverage area at a slower application speed can likely be explained by the difference in number of cells tested at the slower speed.

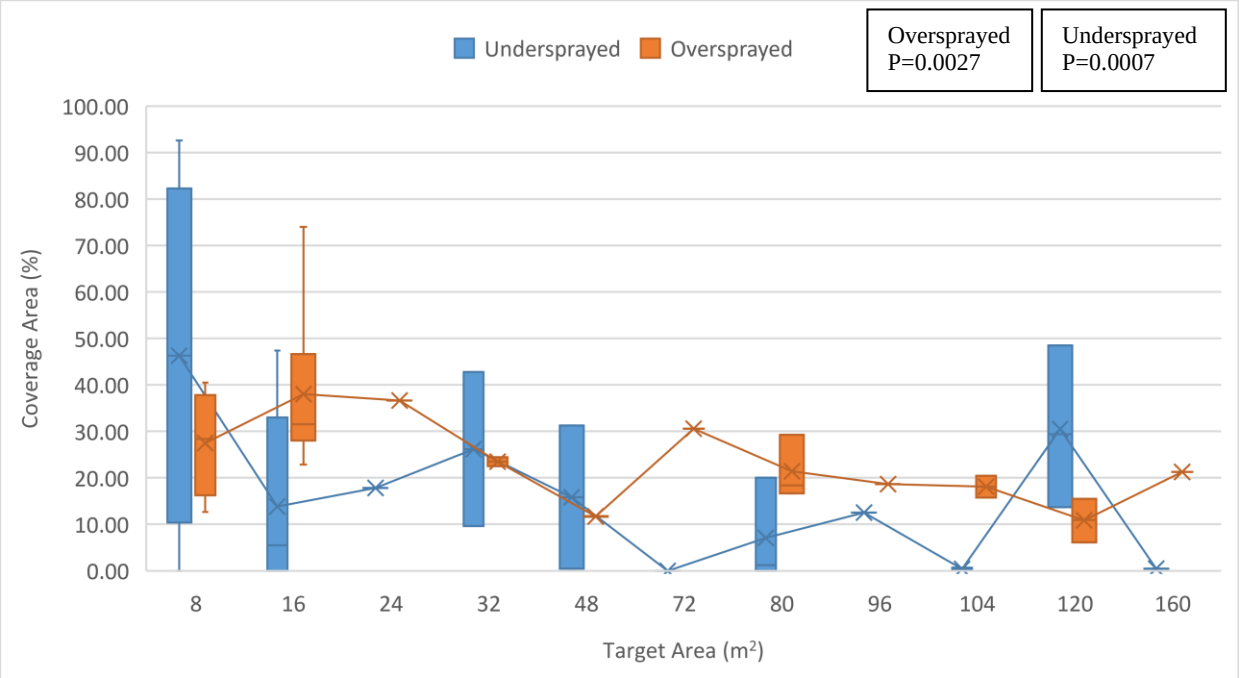

Figure 12. Spray coverage area accuracy percentage by target cell area for field trial 1. Conducted using a Case IH Patriot 4440 and a prescription map with software varied target areas. Each box presents the distribution of coverage area percentage values from 1 to 7 replications.

According to Table 5 and Figure 11, overspray percentage decreased from 27.5% to 21.3%, a 6.2% reduction, and underspray percentage decreased from 46.3% to 0.43%, a 45.8% reduction, which occurred at 8 to 160 m^2 [86.1 to 1722.2 ft^2]. Those differences were statistically significant for both overspray (p=0.0027) and underspray (p=0.0007) with respect to target area.

Both the overspray and underspray percentage areas trended towards decreasing as the cell size target area increased. Although there was no experimental control on the widths and lengths during the initial field trial because it utilized the prescription maps that the SMS Advanced software modified, the results show that the control system accuracy increases as the target area increased. This result is likely because a larger area increases the likelihood of spray being applied within the increased boundary area. However, for the intended method of implementing SSWM that this study is geared towards, larger cell sizes increase the likelihood of weed presence within

the cell when creating the prescription map based on UAS imagery. This in turn would require a larger total area of the field to be sprayed, reducing the effectiveness of the SSWM method.

4.2. Final Test Cell Size and Application Speed Evaluation

The second and final field test as-applied maps were compared to the prescription maps and data were collected. Using information from both maps, values for dependent variables actual coverage, overspray coverage, undersprayed area, and oversprayed area were calculated for each cell. Percentage area values were calculated from the undersprayed area and oversprayed area, the focus of this study. Of the dependent variables, underspray is considered the most critical variable due to the nature of this study. The main concerns with underapplication of herbicide are weed resistance development and allowing the weed seed bank to increase, both leading to greater weed problems in future years (Blackshaw et al., 2006). During the cell width tests, the treatments were the cell widths (SW, MW, and LW), as speed was kept constant at 10.3 km h^{-1} [6.4 mph] and length was kept constant at 3.05 m [10 ft]. Each cell size was tested under the same operating conditions and in the same pass. Table A9, in the appendix, shows the average coverage areas and the means of coverage percentage differences among the cell widths.

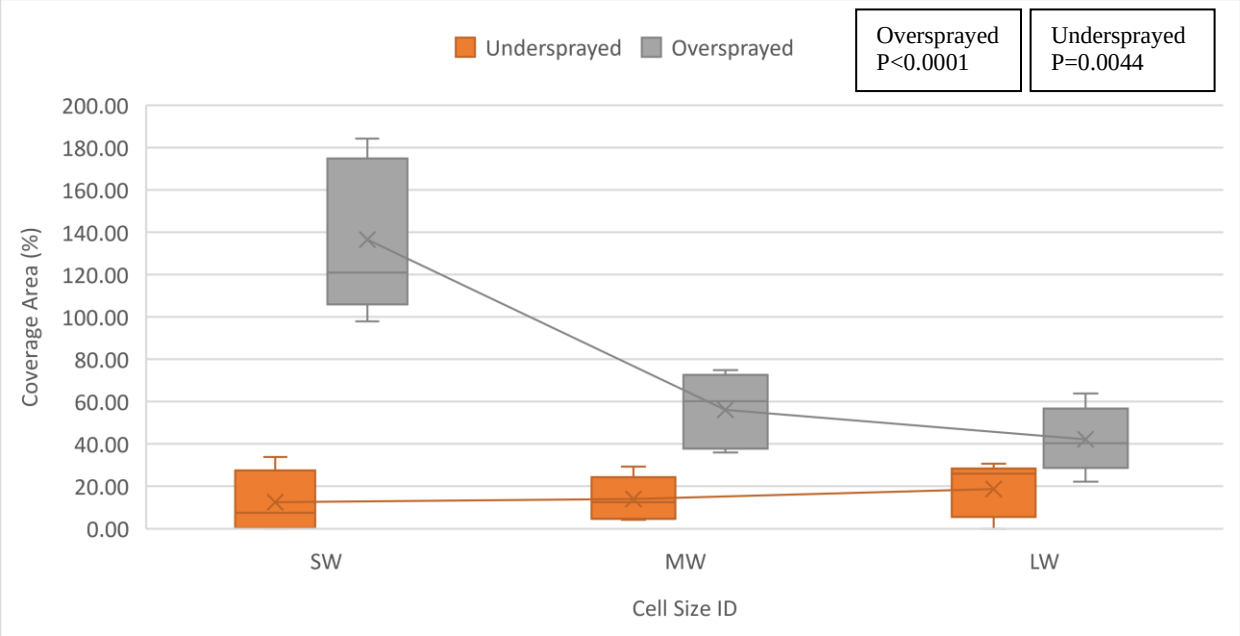

Figure 13. Spray coverage area accuracy percentage by cell width (SW=0.5 m, MW=1.5 m, and LW=3 m) for the final trial. Conducted using a Case IH Patriot 4440 and a prescription map. Each box represents the distribution of coverage area percentage values in 30 replications for each cell width.

According to Figure 13, overspray percentage decreased from 136.5% to 42.2%, a 94.2% reduction, and underspray percentage increased from 12.5% to 18.7%, a 6.2% increase, when the cell width changed from 0.5 to 3 m [1.64 to 9.84 ft]. The percentage coverage areas for overspray ($p<0.0001$) and underspray ($p=0.0044$) were statistically significant with respect to change in cell width.

The trends shown in Figure 13 confirm that the overspray decreases with the increase in width. This is likely the result of the sprayer not being exactly lined up with the smallest width cell so that only one nozzle is activated when required. A notable reduction in overspray is observed for the 1.5 m cell width that adds the width required for two additional nozzles to be activated. With few statistical differences between the 1.5 m and 3 m width cells accuracy and the fact that the 1.5 m width has 4% better percent underspray, it is much more practical and efficient to use that width to take advantage of the SSWM method. The further reduction in percent overspray for

the largest cell width (an additional 2 activated nozzles) doesn't make up for the poorer underspray performance. From a practical standpoint, due to the relationship between cell width and area, the medium cell width (1.5 m) is the best choice to avoid possibility of having to spray more area than required to cover the weeds.

Several factors in addition to the cell width can lead to a cell being oversprayed or undersprayed. These factors include application speed, control system cycle rate, and physical location of the sprayer in relation to the cell. In the case of the smallest cell width (0.5 m) the spray must be exactly lined up with cell to avoid activating two nozzles when only one is intended to be activated, resulting in overspray of twice the area of the cell. Wider cells would likely limit the chance of this occurring as the sprayer doesn't need to be exactly lined up with cell. The speed and refresh rate of the controller determine overspray and underspray in the longitudinal direction, for this reason the speed was constant for the width testing. It is also possible that the method of using a fixed boundary distance to limit the area of interest (AOI) outside the target cells is influencing the results as the AOI is a larger percentage of the target area for the smallest cells (SW=0.5 m) than the larger cells (XL=6.1 m).

The dye solution application to study the effect of cell length and speed on the spraying accuracy was carried out on two back-to-back passes, to provide space in the field for the sprayer to change speeds, on the first pass, and to reach the second treatment speed at the desired stabilized speed. The maps from each pass were combined for analysis, Table 6 summarizes the average coverage areas and the means of percentage difference among the cell lengths and spraying speeds.

Table 6. Summary of the evaluation of field spraying accuracy using a Case IH Patriot 4440 and a prescription map with variable cell length and application speed as input. Cell width were kept constant (7.5 m).

Speed (km h^{-1})	Target Area (m^2)	Average Actual Coverage (m^2)	Average Overspray Coverage (m^2)	Undersprayed % Area	Oversprayed % Area
---------- 7.1 km h^{-1} ----------					
SL (1.5 m long)	11.43	9.818	9.469	14.1	82.84
ML (3.1 m long)	22.86	21.524	13.139	5.84	57.48
LL (4.6 m long)	34.29	32.434	12.82	5.41	37.39
XL (6.1 m long)	45.72	44.134	12.197	3.47	26.68
---------- 10.3 km h^{-1} ----------					
SL (1.5 m long)	11.43	7.318	6.418	35.98	56.15
ML (3.1 m long)	22.86	18.896	8.418	17.34	36.82
LL (4.6 m long)	34.29	30.346	8.843	11.5	25.79
XL (6.1 m long)	45.72	40.56	5.224	11.29	11.43
---------- 13.5 km h^{-1} ----------					
SL (1.5 m long)	11.43	3.468	7.98	69.66	69.82
ML (3.1 m long)	22.86	16.14	7.155	29.4	31.3
LL (4.6 m long)	34.29	27.368	6.792	20.19	19.81
XL (6.1 m long)	45.72	36.31	4.316	20.58	9.44

Each line contains the average of 5 treatment replications.

Once again, due to a lack of repetitions completed the spraying speed tests are not valid, however general trends observed, that are in no way significant, can be discussed. Spraying speed and cell length were linked due to the physical limitations of sections of the spray boom not being able to vary speed across its length when traveling in a straight path. However, further testing could reduce the variance observed in this study. Figure 14 displays the overspray and underspray trends with change in spraying speed. Tables 7 and 8, summarize the type 3 tests of fixed effects on underspray percentage area and overspray percentage area respectively.

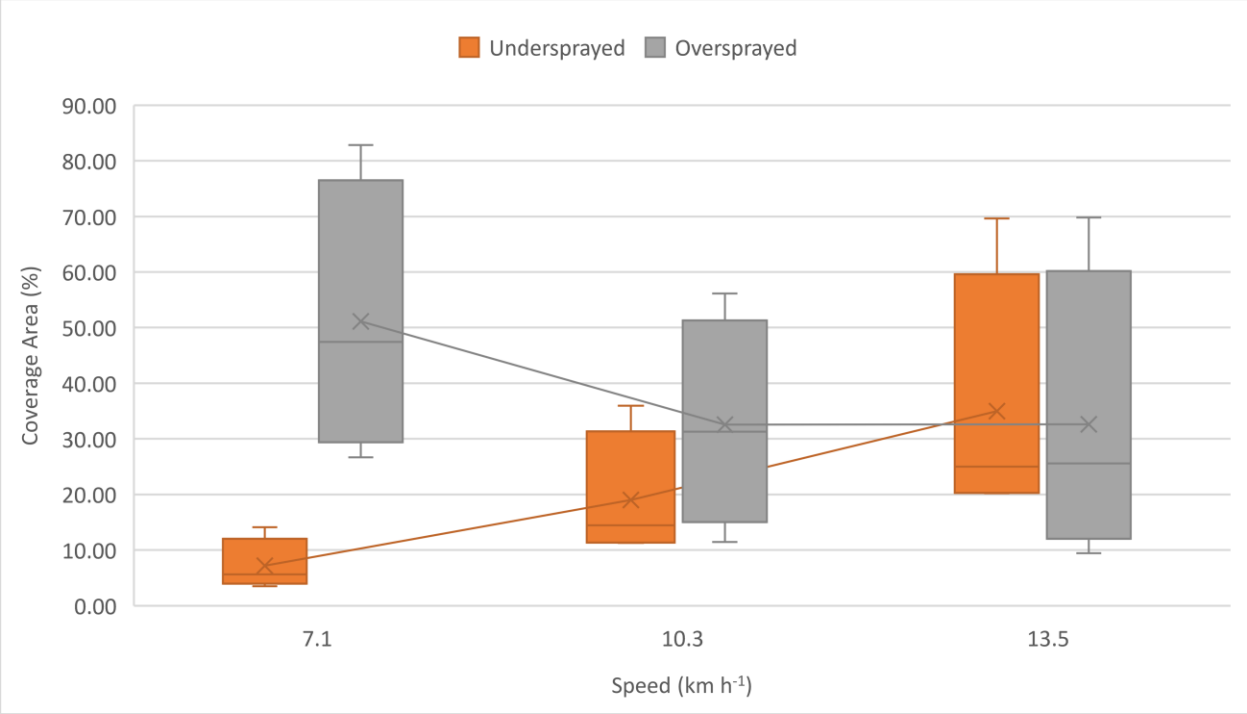

Figure 14. Spray coverage area accuracy percentage by application speed for the final trial. Conducted using a Case IH Patriot 4440 and a prescription map applicated at three speeds. Each box represents the distribution of coverage area percentage for 20 replications (4 cell lengths).

According to Table 6 and Figure 14, overspray percentage decreased from 51.1% to 32.6%, a 18.5% reduction, and underspray percentage increased from 7.2% to 35.0%, a 27.7% increase, which occurred at speeds 7.1 to 13.5 km h^{-1} [4.4 to 8.4 mph]. The underspray percentage area trended towards increasing as spraying speed increased, tending to agree with the trend from the first trial. The overspray percentage area trended towards decreasing and then levelled off as spraying speed increased.

The variability in the data shown for application speed testing is likely the direct result of four different cell lengths in each speed range, a byproduct of the randomized block design combined over speeds for this portion of the study. Because two variables were tested at the same time an increase in errors occurred as the different cell sizes were likely affected by the speed in different ways. However, there is still an identifiable trend, which is that at slower speeds

underspray is reduced, but overspray is increased. The underspray trend to increase as the spraying speed increased is likely a direct response to the system refresh rate. At the same time, the overspray decreased before leveling off, the reasons for such behavior remain unclear at this point. To use these results to determine the optimum speed, the use case for this study must be acknowledged. Productivity, or acres sprayed per hour, must be considered along with the accuracy results as adoption of this SSWM method and its success will ultimately be decided by the producers who intend on implementing the weed control method on their operation.

Due to this, the application speed of 10.3 km h^{-1} (6.4 mph) was selected as the optimum application speed because it offers better underspray performance than the faster speed and better overspray performance than the slower application speed. Even though the slower application speed offers better underspray performance, the reduction in acres sprayed per hour does not warrant its selection.

A likely contributing factor to a cell being oversprayed or undersprayed is the control system refresh rate. In the case of this study, the control system refreshed at 10 Hz and depending on the application speed a significant amount of ground was covered during the time between nozzle on and nozzle off signals. For the speeds studied, 0.19 to 0.38 m (0.65 to 1.23 ft) could be travelled in the time between the controller sending an on or off signal. Using the most extreme scenarios studied, the smallest length (SL=1.52 m) sprayed at the fastest speed (13.5 km h^{-1}) was covered in as little as 0.77 seconds, while it took 3.1 seconds to cover the largest length (XL=6.1 m) when it was sprayed at the slowest speed (7.1 km h^{-1}). The fastest application speed and the smallest length resulted in very poor application accuracy and offered some validity to the Case IH engineer's recommendations of applicating no faster than 1 foot every tenth of a second. A longer cell would allow for more time and distance to be covered without the controller missing

an input and therefore accuracy would likely improve. Table 7 below begins the cell length treatment analysis.

Table 7. Type 3 tests of fixed effects on underspray percentage area for a field trial conducted using a Case IH Patriot 4440 and a prescription map.

Effect	Num DF	Den DF	F Value	Pr > F
Speed	2	12	7.12	0.0092
Length	3	36	25.36	<0.0001
Length*Speed	6	36	4.4	0.002

Table 8. Type 3 tests of fixed effects on overspray percentage area for a field trial conducted using a Case IH Patriot 4440 and a prescription map.

Effect	Num DF	Den DF	F Value	Pr > F
Speed	2	12	7.17	0.0089
Length	3	36	35.47	<0.0001
Length*Speed	6	36	0.59	0.7395

The highlighted value on Table 7 shows that Length times Speed component was found significant for underspray percentage accuracy, thus the effect of length depended on spraying speed and vice versa. The interaction was evaluated by slicing the test based on speed, summarized in Table 9, and resulting in Figure 15 below. However, the highlighted values on Table 8 shows length was the only significant factor on overspray percentage accuracy and the spraying speed did not influence the effect of length, summarized in Table 10, and resulting in Figure 16 below.

Table 9. Summary of effect of relative plot size on proportion of percent underspray for three increasing rates of spraying speed. Conducted using a Case IH Patriot 4440 and a prescription map.

	Proportion % of Intended Area Undersprayed ---------- m^2 m^{-2} *100 ----------				
	Spraying Speed ---------- km h^{-1} (mph) ----------				
Plot Size	7.1 (4.4)	10.3 (6.4)		13.5 (8.4)	
SL	14.10	35.98	b_z	69.66	b
ML	05.84	17.34	a	29.40	a
LL	05.41	11.50	a	20.19	a
XL	03.57	11.29	a	20.58	a
p-value$_y$	0.3754$_x$	0.0012		<0.001	

$_x$ - mean separation was not complete for speeds not having significant variance at $\alpha = 0.05$
$_y$ - p-value of a test of simple effects plot size within spray speeds.
$_z$ - means within the same speed having the same letter are not statistically different at $\alpha = 0.05$

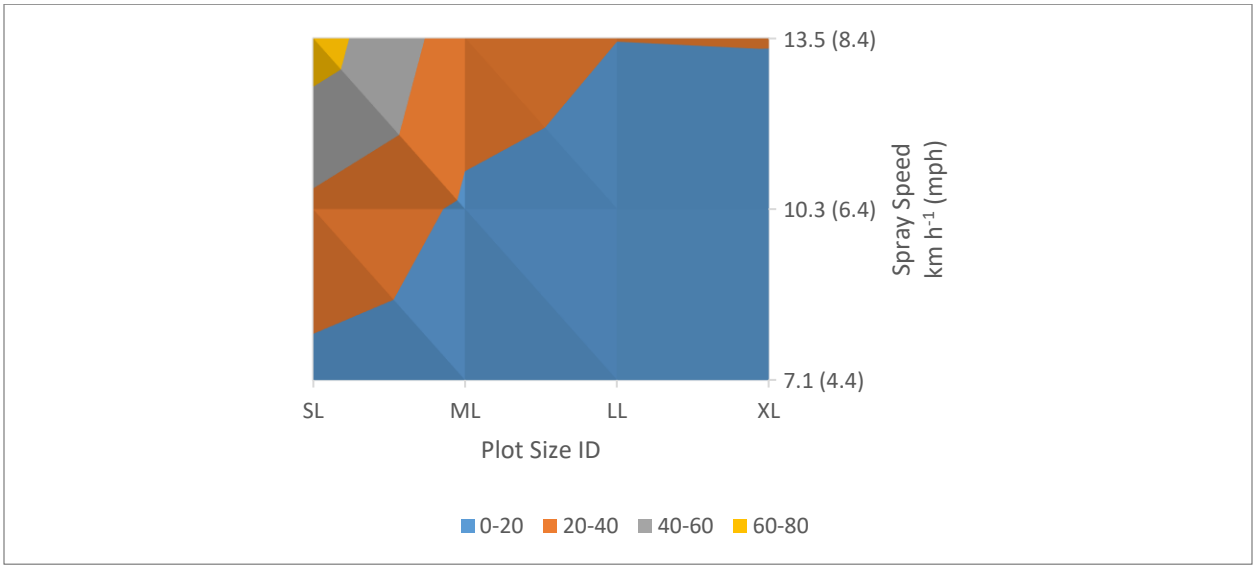

Figure 15. Proportion of percentage underspray coverage area trends across plots (SL=1.5 m, ML=3.1 m, LL=4.6 m, and XL=6.1 m) and spray application speeds for the final trial. Conducted using a Case IH Patriot 4440 and a prescription map.

According to Table 9 and Figure 15, as spraying speed increases the differences trend towards increasing as well. Within the individual spraying speeds, the smallest length treatment had the highest percentage of undersprayed area, and the next three larger lengths had a greatly reduced percentage of undersprayed area. The three large length treatments performed better than

the smallest length treatment and had no difference within the 10.3 km h^{-1} (6.4 mph) speed. Similarly, the three larger length treatments within the 13.5 km h^{-1} (8.4 mph) speed, performed better than the smallest length treatment and also had no difference. Predictably, the smallest treatment sprayed at the fastest speed had the highest percentage of undersprayed area (Figure 15).

Table 10. Summary of least squares means of overspray percentage area with change in length (SL=1.5 m, ML=3.1 m, LL=4.6 m, and XL=6.1 m). Conducted using a Case IH Patriot 4440 and a prescription map.

Plot Size	Proportion % of Intended Area Oversprayed ---------- m^2 m^{-2} *100 ----------	
SL	69.60	c_z
ML	41.87	b
LL	27.66	ab
XL	15.85	a
p-value	<0.0001	

z – means followed by the same letter are not statistically different based on an f-protected pairwise-t-test

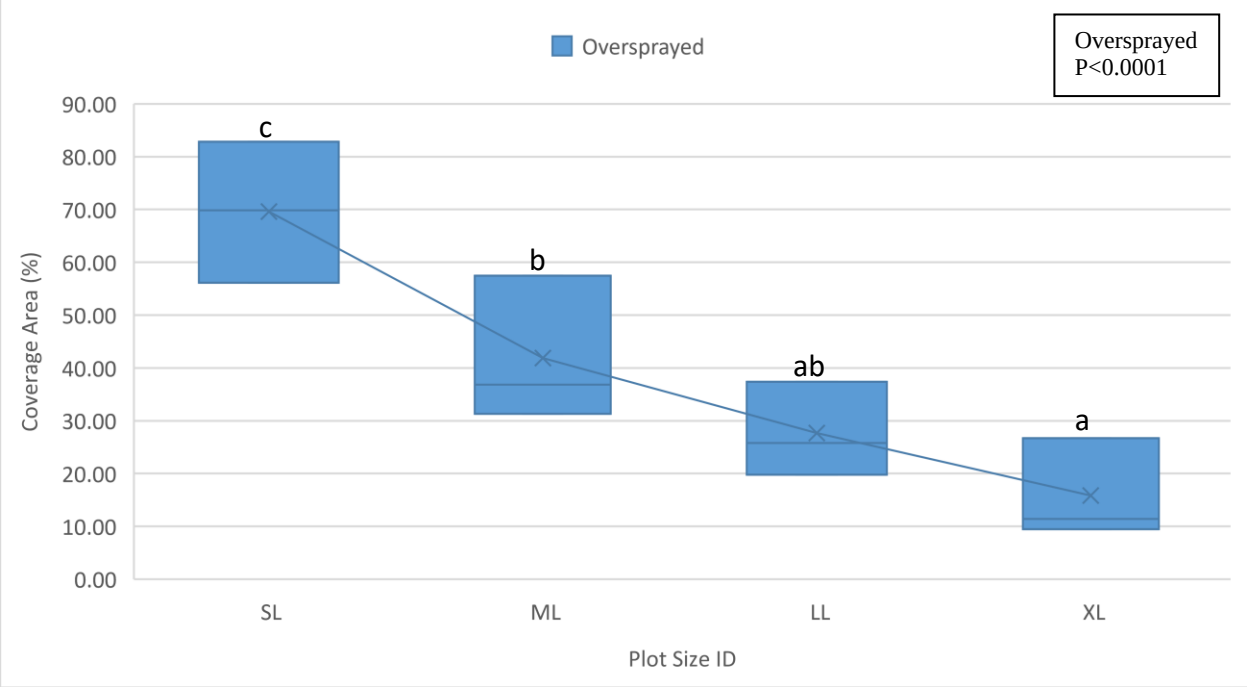

Figure 16. Effect of cell length (SL=1.5 m, ML=3.1 m, LL=4.6 m, and XL=6.1 m) on the percent overspray of coverage area for the final trial. Conducted using a Case IH Patriot 4440 and a prescription map. Plot mean values having the same letter are not statistically different based on an f-protected pairwise t-test.

According to Table 10 and Figure 16, overspray percentage decreased from 69.6% to 15.9%, a 53.7% decrease, which occurred at lengths 1.52 to 6.10 m [5 to 20 ft]. The percentage coverage area for overspray ($p<0.0001$) was statistically significant with respect to change in treatment length. With this significance, it can be concluded that the cell length influences the spray accuracy and there is an identifiable trend in the data that shows an increase in length causes a reduction in percent overspray.

It is interesting to note that the spraying speed showed interaction with the cell length when looking at percentage underspray, but for percentage overspray, cell length was the only significant factor and speed did not influence the effect of length. It is not understood at this time why this is the case, but further study will likely shed more light on this.

To make the optimum cell length recommendation, the practicality of implementing the cell lengths was considered. SSWM works best by matching the variability of the weed presence in the field and a smaller cell length would increase the resolution the of prescription map allowing it to follow the weed distribution more closely, increasing the likelihood of cost savings when compared with a blanket herbicide application. That said, at first glance it would make sense to opt for the SL length, since there is no significant difference among the cell lengths but Figures 15 and 16 showed a trend for higher underspray and overspray when using that cell length. Still on Figure 15, the results show a decrease in both underspray when going from SL to ML cell lengths, and the underspray levels off for the other two cell lengths. Given that the under-application of herbicide is more concerning than over-application, because of potential development of herbicide-resistant weeds (Blackshaw et al., 2006), the ML treatment length (3.05 m [10 ft]) was selected as the optimum cell length because it minimizes underspray in relation to the SL treatment and has similar overspray rates to the other larger cell lengths. Also, it impacts the effectiveness

of the SSWM application by likely reducing the amount of chemical applied compared to the larger cell lengths.

A possible cause for the variability is the size of the area of interest placed around each test cell. The chosen width of 0.25 m to each (North-South) side and 0.75 m (East-West) end effectively doubles the area of the smallest width testing cell whereas it has a much smaller area percentage for the largest of the length testing cells. Once again, these constraints were chosen based on the spacing between target cells.

4.3. Cell Size Evaluation

The comparison between different cell widths, lengths, and application speeds were conducted to determine possible interactions of these dependent variables on spray application accuracy. The results from the combination of the two field tests shows that dependent variable with the largest statistical effect on spray application accuracy is cell width followed by cell length. As the speed testing did not have a sufficient number of replicates, the speed recommendation is based on practicality and industry guidance partially backed up by the insignificant data trends. The results show that the optimum cell size and speed for the sprayer system tested is a cell size of 1.5 x 3.05 m [4.92 x 10 ft] applied at a speed of 10.3 km h^{-1} [6.4 mph]. The combination of this width, length and application speed reduces the spray placement inaccuracies by minimizing the under-spray and the overspray and offers the best performance without compromising on the number of acres sprayed per hour. However, statistical significance could be further improved. It is also important to note that the cell length and application speed recommendations could likely be different for a control system, both GPS receiver and nozzle actuators, that operates at a higher refresh rate. A higher refresh rate would likely allow for either a smaller cell length, a faster application speed, or some combination of both.

Even though cell length results did not show statistical significance with regards to spray accuracy, recommended cell length must be considered due its effect on prescription map resolution because resolution directly correlates to how much of the field is identified for spraying. A smaller length correlates to an increased resolution for the prescription map because the cells are smaller, which in turn, results in a prescription map that more closely follows the weed distribution present in the field. This is because the larger a cell is (area), the higher the likelihood of a weed being present within cell is, thereby identifying the complete area for spray application. Just one identified weed being present anywhere within a cell on the prescription map identifies that entire cell area for spraying, so the potential for overapplication on areas with no weed presence increases. Therefore, to take advantage of the benefits of site-specific weed management, the cell size used for creating the prescription map should be kept as small as possible while still guaranteeing accurate targeting by the sprayer system.

The outcomes of field testing the cell sizes are indicative of some of the limitations of the current nozzle control technology for the specific spray control system used. The main limitation of this study was the size and scope of the field trials. A larger test would likely level out some of the random errors that can affect smaller field trials, such as the small field trial this project covers. Larger field trials would likely better simulate actual operating conditions and allows the sprayer systems to further stabilize during application.

5. CONCLUSION

In this project, various cell sizes (widths and lengths) were tested using a prescription map to simulate different conditions for site-specific weed control and to evaluate the accuracy to spray operation across those cell sizes under three different application speeds. The cell sizes were tested by comparing the prescription maps to the as-applied maps to evaluate the performance of the spraying operation. The field test results showed that the dependent variable cell width had the greatest effect on application accuracy (p-values < 0.05). However, cell length had an identifiable effect on application accuracy to a lesser extent but is still important to the implementation and effectiveness of SSWM. Although spraying speed tests didn't have the required replicates for significance an accuracy trend was observed. Results showed that an optimum cell size with a width of 1.5 m [4.92 ft] and a length of 3.05 m [10 ft] should be used when creating the SSWM prescription maps. In addition, spray application should be made at a speed of 10.3 km h^{-1} [6.4 mph].

6. RECOMMENDATIONS FOR FUTURE STUDIES

Cell width, application speed, and cell length are all affecting the accuracy of the spray application. Due to application speed being a significant contributing factor in this regard, to improve the accuracy and coverage of herbicide application using a prescription map for SSWM, it is important to conduct more field tests with a variety of manufacturers and equipment. In order to minimize any random errors, the cell size field testing needs to be expanded and cell sizes and distributions should be further randomized to simulate actual SSWM field conditions. In addition, as a result of the optimum cell width and cell length being different dimensions, an increased awareness in route planning is needed.

Selecting an effective dye as an indicator could further refine the analysis by using UAS imagery, versus relying on the system generated as-applied maps which could have system lag time bias represented and differences in geolocation. Alternatively, instead of using a spray indication dye, this study could be carried out by planting a crop easily killed by an herbicide, applying the herbicide, and then flying the test area several days after herbicide application would also allow for the use of UAS imagery for analysis.

Based on the constraints of this study, it is recommended to use a cell size with a width of 1.5 m [4.92 ft] and a length of 3.05 m [10 ft] for prescription maps and apply at a speed of 10.3 km h^{-1} [6.4 mph]. In addition to that, it would be more realistic to conduct a truly randomized approach to cell size and placement that more closely resembles the patchy weed distribution observed in production agriculture, which would significantly add to the robustness of this study. Another gap that could be addressed with future testing is to investigate how total system load affects the accuracy, that is, how accuracy is affected by percentage of nozzles in use at any given time. A final gap that could be explored is how route planning affects accuracy. Examples of this

could be how centered on the cells does the sprayer need to be or how going against the intended direction of travel (for rectangular cells) affects the spray application accuracy.

REFERENCES

Al-Gaadi, K. A., & Ayers, P. D. (1999). Integrating GIS and GPS into a spatially variable rate herbicide application system. *Applied Engineering in Agriculture*. 15(4), 255–262.

Ayers, P. D., Rogowski, S. M., & Kimble, B. L. (1990). An investigation of factors affecting sprayer control system performance. *Applied Engineering in Agriculture*. 6(6), 701–706.

Blackshaw R. E., O'donovan, J.T., Harker, K. N., Clayton, G. W., & Stougaard, R. N. (2006). Reduced herbicide doses in field crops: A review. *Weed Biology & Management, 6*(1), 10-17. https://doi-org./10.1111/j/1445-6664.2006.00190.x

Bolat, A., & Özlüoymak, Ö. B. (2020). Evaluation of performances of different types of spray nozzles in site-specific pesticide spraying. *Semina: Ciências Agrárias*, *41*(4), 1199. https://doi.org/10.5433/1679-0359.2020v41n4p1199

Bosch. (2020). Smart spraying – precision herbicide application on weeds. *Bosch.* Retrieved from: https://www.bosch.com/research/know-how/success-stories/smart-spraying-precision-herbicide-application-on-weeds/

CaseIH. (2020). Patriot Series Sprayer. In *Get ultimate spray control with AIM Command FLEX*. Retrieved from: https://www.caseih.com/northamerica/en-us/products/application-equipment/patriot-series-sprayers

Christensen, S., Søgaard, H. T., Kudsk, P., Nørremark, M., Lund, I., Nadimi, E. S., & Jørgensen, R. (2009). Site-specific weed control technologies. *Weed Research*, *49*(3), 233–241. https://doi.org/10.1111/j.1365-3180.2009.00696.x

Cossette, M. (2019). Precision agriculture technology adoption and usage in North Dakota. MS thesis. Fargo, North Dakota. North Dakota State University, Department of Agribusiness and Applied Economics.

Fultz, A. (2018). Flying ahead of the pack: Drones in the agriculture industry. *Computer & Internet Lawyer.* 35(4), 1–4.

Gašparović, M., Zrinjski, M., Barković, Đ., & Radočaj, D. (2020). An automatic method for weed mapping in oat fields based on UAV imagery. *Computers and Electronics in Agriculture, 173,* 105385. https://doi.org/10.1016/j.compag.2020.105385

Gerhards, R., & Oebel, H. (2006). Practical experiences with a system for site-specific weed control in arable crops using real-time image analysis and GPS-controlled patch spraying. *Weed Research, 46*(3), 185–193. https://doi.org/10.1111/j.1365-3180.2006.00504.x

Ghasemzadeh, H. R., & Humburg, D. D. (2016). Using variable spray angle fan nozzle on long spray booms. *Agric Eng Int: CIGR Journal,* 18(1), 82-90. http://www.cirgrjournal.org

Hengl, T. (2006). Finding the right pixel size. *Computers and Electronics in Agriculture.* 32, 1283–1298.

Hollis, P. (2011). Precision ag helps in resistant weed battle. *Southeast Farm Press.*

Hong, S., Minzan, L., & Zhang, Q. (2012). Detection system of smart sprayers: Status, challenges, and perspectives. *Int J Agric & Biol Eng, 5(3),* 10-23. https://doi.org/10.3965/j.ijabe.20120503.002

Huang, H., Deng, J., Lan, Y., Yang, A., Deng, X., Wen, S., Zhang, H., & Zhang, Y. (2018). Accurate Weed Mapping and Prescription Map Generation Based on Fully Convolutional Networks Using UAV Imagery. *Sensors*, *18*(10), 3299. https://doi.org/10.3390/s18103299

Huang, H., Lan, Y., Yang, A., Zhang, Y., Wen, S., & Deng, J. (2020). Deep learning versus Object-based Image Analysis (OBIA) in weed mapping of UAV imagery. *International Journal of Remote Sensing*, *41*(9), 3446–3479. https://doi.org/10.1080/01431161.2019.1706112

Hunter, J. E., Gannon, T. W., Richardson, R. J., Yelverton, F. H., & Leon, R. G. (2020). Integration of remote-weed mapping and an autonomous spraying unmanned aerial vehicle for site-specific weed management. *Pest Management Science*, *76*(4), 1386–1392. https://doi.org/10.1002/ps.5651

Jurado-Expósito, M., López-Granados, F., García-Torres, L., García-Ferrer, A., Sánchez de la Orden, M., & Atenciano, S. (2003). Multi-species weed spatial variability and site-specific management maps in cultivated sunflower. *Weed Science*. 51, 319–328.

Kamilaris, A., & Prenafeta-Boldú, F. X. (2018). Deep learning in agriculture: A survey. *Computers and Electronics in Agriculture*, *147*, 70–90. https://doi.org/10.1016/j.compag.2018.02.016

Kirkpatrick, K. (2019). Technologizing agriculture: An array of technologies are making farms more efficient, safer, and profitable. *Communications of the ACM.* 62(2), 14–16.

Laws, F. (2004). Trimble offers new lightbar guidance system. *Southwest Farm Press* 31(3), 23–23.

López-Granados, F. (2011). Weed detection for site-specific weed management: Mapping and real-time approaches: Weed detection for site-specific weed management. *Weed Research*, *51*(1), 1–11. https://doi.org/10.1111/j.1365-3180.2010.00829.x

López-Granados, F., Torres-Sánchez, J., Serrano-Pérez, A., de Castro, A. I., Mesas-Carrascosa, Fco.-J., & Peña, J. M. (2016). Early season weed mapping in sunflower using UAV technology: Variability of herbicide treatment maps against weed thresholds. *Precision Agriculture*, *17*(2), 183–199. https://doi.org/10.1007/s11119-015-9415-8

Luck, J., Pitla, S., Shearer, S., Mueller, T., Dillon, C.R., Fulton, J., & Higgins, S. (2010). Potential for pesticide and nutrient savings via map-based automatic boom section control of spray nozzles. *Computers and Electronics in Agriculture*. 70, 19-26. 10.1016/j.compag.2009.08.003.

Luck, J., Stombaugh, T., and Shearer, S. (2011). Basics of automatic section control for agricultural sprayers. *Cooperative Extension Service University of Kentucky College of Agriculture.* http://www2.ca.uky.edu/agcomm/pubs/aen/aen102/aen102.pdf.

Marc-André Michaud, Chris Watts, & David Percival. (2006). Precision Pesticide Delivery Based on Aerial Spectral Imaging. *2006 CSBE/SCGAB, Edmonton, AB Canada, July 16-19, 2006*. 2006 CSBE/SCGAB, Edmonton, AB Canada, July 16-19, 2006. https://doi.org/10.13031/2013.22081

Marsh, A. (2018). John Deere and the birth of precision agriculture. *IEEE Spectrum*. https://spectrum.ieee.org/tech-history/silicon-revolution/john-deere-and-the-birth-of-precision-agriculture

Mid-South AG Equipment. (2020). *Shop Raven Viper4+*. Retrieved from: https://shop.midsouthag.com/products/raven-viper-4-with-gps-mba-6-antenna-117-5010-010w

Nalavade, P. P., V. M. Salokhe, H. P. W. Jayasuriya, and H. Nakashima. (2008). Development of a tractor mounted wide spray boom for increased efficiency. *Journal of Food, Agriculture & Environment*, 6(2), 164-169.

Peña, J. M., Torres-Sánchez, J., de Castro, A. I., Kelly, M., & López-Granados, F. (2013). Weed Mapping in Early-Season Maize Fields Using Object-Based Analysis of Unmanned Aerial Vehicle (UAV) Images. *PLoS ONE, 8*(10), e77151. https://doi.org/10.1371/journal.pone.0077151

Rasmussen, J., Azim, S., Nielsen, J., Mikkelsen, B. F., Hørfarter, R., & Christensen, S. (2020). A new method to estimate the spatial correlation between planned and actual patch spraying of herbicides. *Precision Agriculture, 21*(4), 713–728. https://doi.org/10.1007/s11119-019-09691-5

Schimmelpfennig, D. (2016). Farm profits and adoption of precision agriculture. *United States Department of Agriculture*. https://www.ers.usda.gov/webdocs/publications/80326/err-217.pdf?v=0

Sharda, A., Luck, J. D., Fulton, J. P., McDonald, T. P., & Shearer, S. A. (2013). Field application uniformity and accuracy of two rate control systems with automatic section capabilities on agricultural sprayers. *Precision Agriculture, 14*(3), 307–322. https://doi.org/10.1007/s11119-012-9296-z

Torres-Sánchez, J., López-Granados, F., De Castro, A. I., & Peña-Barragán, J. M. (2013). Configuration and Specifications of an Unmanned Aerial Vehicle (UAV) for Early Site Specific Weed Management. *PLoS ONE*, *8*(3), e58210. https://doi.org/10.1371/journal.pone.0058210

Trimble. (2019, October 7). *Trimble launches next-generation WeedSeeker 2 spot spray system.* [Press Release]. Retrieved from https://www.trimble.com/news/release.aspx?id=100719a

Wei, D., Huang, Y., Chunjiang, Z., Xiu, W., & Jinlong, L. (2013). Spatial distribution visualization of PWM continuous variable-rate spray. *Int J Agric & Biol Eng*, 6(4), 1-8. https://doi.org/10.3965/j.ijabe.20130604.001

Wei, D., Xiongkui, H., & Weimin, D. (2009). Droplet size and spray pattern characteristics of PWM-based continuously variable spray. *Int J Agric & Biol Eng*, 2(1), 8-18. https://doi.org/10.3965/j.issn.1934-6344.2009.01.008-018

Xu, Y., Gao, Z., Khot, L., Meng, X., & Zhang, Q. (2018). A Real-Time Weed Mapping and Precision Herbicide Spraying System for Row Crops. *Sensors*, *18*(12), 4245. https://doi.org/10.3390/s18124245

Yang, C., Everitt, J., Du, Q., Luo, B., and Chanussot, J. (2013). Using high-resolution airborne and satellite imagery to assess crop growth and yield variability for precision agriculture. *IEEE.* https://ieeexplore-ieeeorg.ezproxy.lib.ndsu.nodak.edu/stamp/stamp.jsp?tp=&arnumber=6236221

Zhang, N., Wang, M., & Wang, N. (2002). Precision agriculture—A worldwide overview. *Computers and Electronics in Agriculture*, *36*(2–3), 113–132. https://doi.org/10.1016/S0168-1699(02)00096-0

APPENDIX

Table A1. Initial trial raw test results.

Cell ID	Speed (km h^{-1})	Tgt. Area	Spray Cvg. Area	% Sprayed	% Underspray	Overspray Cvg. Area	% Overspray	% Diff.
1	10.3	8	3.91	48.88	51.13	3.24	40.50	91.63
3	10.3	8	4.68	58.50	41.50	2.38	29.75	71.25
5	10.3	8	0.59	7.38	92.63	1.01	12.63	105.25
8	10.3	8	8.00	100.00	0.00	2.16	27.00	27.00
2	10.3	16	8.42	52.63	47.38	4.48	28.00	75.38
14	10.3	16	16.00	100.00	0.00	3.66	22.88	22.88
17	10.3	16	10.72	67.00	33.00	4.71	29.44	62.44
20	7.1	16	15.12	94.50	5.50	5.05	31.56	37.06
21	7.1	16	14.46	90.38	9.63	5.41	33.81	43.44
23	7.1	16	15.81	98.81	1.19	7.46	46.63	47.81
27	7.1	16	16.00	100.00	0.00	11.84	74.00	74.00
25	7.1	24	19.73	82.21	17.79	8.79	36.63	54.42
7	10.3	32	18.32	57.25	42.75	7.21	22.53	65.28
26	7.1	32	28.92	90.38	9.63	7.83	24.47	34.09
4	10.3	48	33.01	68.77	31.23	5.63	11.73	42.96
19	7.1	48	47.78	99.54	0.46	5.58	11.63	12.08
9	10.3	72	72.00	100.00	0.00	21.99	30.54	30.54
15	10.3	80	80.00	100.00	0.00	23.43	29.29	29.29
16	10.3	80	63.96	79.95	20.05	14.69	18.36	38.41
24	7.1	80	79.05	98.81	1.19	13.32	16.65	17.84
10	10.3	96	84.00	87.49	12.51	17.88	18.62	31.13
13	10.3	104	103.88	99.88	0.12	16.38	15.75	15.87
22	7.1	104	103.29	99.31	0.69	21.25	20.43	21.12
11	10.3	120	61.85	51.54	48.46	7.33	6.11	54.57
12	10.3	120	84.71	70.59	29.41	13.09	10.91	40.32
18	7.1	120	103.61	86.33	13.67	18.6	15.50	29.16
6	10.3	160	159.32	99.57	0.43	34.03	21.27	21.70

Table A2. Second and final trial raw cell width testing results for 0.5 m.

Group	Cell ID	Spray Cvg. Area	% Sprayed	% Underspray	Overspray Cvg. Area	% Overspray	% Difference
	SW1	1.49	97.77	2.23	1.448	95.01	97.24
	SW2	1.524	100.00	0.00	2.251	147.70	147.70
1	SW3	1.524	100.00	0.00	2.036	133.60	133.60
	SW4	1.524	100.00	0.00	2.036	133.60	133.60
	SW5	1.524	100.00	0.00	2.036	133.60	133.60
	SW6	1.524	100.00	0.00	1.253	82.22	82.22
	SW7	0.06	3.94	96.06	2.32	152.23	248.29
	SW8	1.47	96.46	3.54	1.7925	117.62	121.16
2	SW9	1.43	93.83	6.17	1.8075	118.60	124.77
	SW10	1.43	93.83	6.17	1.8225	119.59	125.75
	SW11	1.42	93.18	6.82	1.8275	119.91	126.74
	SW12	1.41	92.52	7.48	0.86	56.43	63.91
	SW13	0.2	13.12	86.88	2.32	152.23	239.11
	SW14	1.18	77.43	22.57	1.6	104.99	127.56
3	SW15	1.17	76.77	23.23	1.06	69.55	92.78
	SW16	1.17	76.77	23.23	1.6	104.99	128.22
	SW17	1.17	76.77	23.23	1.62	106.30	129.53
	SW18	1.16	76.12	23.88	0.75	49.21	73.10
	SW19	1.524	100.00	0.00	2.636	172.97	172.97
	SW20	1.524	100.00	0.00	2.766	181.50	181.50
4	SW21	1.524	100.00	0.00	2.846	186.75	186.75
	SW22	1.524	100.00	0.00	2.866	188.06	188.06
	SW23	1.524	100.00	0.00	2.865	187.99	187.99
	SW24	1.524	100.00	0.00	2.864	187.93	187.93
	SW25	1.36	89.24	10.76	2.91	190.94	201.71
	SW26	1.38	90.55	9.45	2.53	166.01	175.46
5	SW27	1.4	91.86	8.14	2.41	158.14	166.27
	SW28	1.42	93.18	6.82	2.41	158.14	164.96
	SW29	1.44	94.49	5.51	2.42	158.79	164.30
	SW30	1.46	95.80	4.20	2.44	160.10	164.30

Trial conducted at 10.3 km h^{-1} [6.4 mph]. Target area 1.52 m^2. Size identifier SW.

Table A3. Second and final trial raw cell width testing results for 1.5 m.

Group	Cell ID	Spray Cvg. Area	% Sprayed	% Underspray	Overspray Cvg. Area	% Overspray	% Difference
	MW1	4.28	93.61	6.39	1.45	31.71	38.10
	MW2	3.95	86.40	13.60	1.66	36.31	49.91
1	MW3	4.33	94.71	5.29	2.215	48.45	53.74
	MW4	4.5	98.43	1.57	1.335	29.20	30.77
	MW5	4.43	96.89	3.11	1.68	36.75	39.85
	MW6	4.52	98.86	1.14	1.54	33.68	34.82
	MW7	4.18	91.43	8.57	1.51	33.03	41.60
	MW8	4.11	89.90	10.10	1.53	33.46	43.57
2	MW9	4.04	88.36	11.64	1.41	30.84	42.48
	MW10	3.97	86.83	13.17	1.44	31.50	44.66
	MW11	3.9	85.30	14.70	1.44	31.50	46.19
	MW12	3.82	83.55	16.45	3.53	77.21	93.66
	MW13	3.28	71.74	28.26	4.524	98.95	127.21
	MW14	3.26	71.30	28.70	3.388	74.10	102.80
3	MW15	3.24	70.87	29.13	2.208	48.29	77.43
	MW16	3.22	70.43	29.57	1.938	42.39	71.96
	MW17	3.2	69.99	30.01	1.818	39.76	69.77
	MW18	3.19	69.77	30.23	2.62	57.31	87.53
	MW19	3.42	74.80	25.20	3.724	81.45	106.65
	MW20	4.572	100.00	0.00	3.724	81.45	81.45
4	MW21	4.572	100.00	0.00	3.724	81.45	81.45
	MW22	4.572	100.00	0.00	3.724	81.45	81.45
	MW23	4.572	100.00	0.00	3.724	81.45	81.45
	MW24	4.572	100.00	0.00	1.91	41.78	41.78
	MW25	3.4	74.37	25.63	3.935	86.07	111.70
	MW26	3.52	76.99	23.01	3.715	81.26	104.27
5	MW27	3.63	79.40	20.60	3.084	67.45	88.06
	MW28	3.75	82.02	17.98	2.816	61.59	79.57
	MW29	3.86	84.43	15.57	2.85	62.34	77.91
	MW30	3.98	87.05	12.95	2.89	63.21	76.16

Trial conducted at 10.3 km h^{-1} [6.4 mph]. Target area 4.57 m^2. Size identifier MW.

Table A4. Second and final trial raw cell width testing results for 3.0 m.

Group	Cell ID	Spray Cvg. Area	% Sprayed	% Underspray	Overspray Cvg. Area	% Overspray	% Difference
	LW1	7.56	82.68	17.32	1.87	20.45	37.77
	LW2	8.56	93.61	6.39	2.208	24.15	30.53
1	LW3	8.29	90.66	9.34	3.076	33.64	42.98
	LW4	7.94	86.83	13.17	2.546	27.84	41.01
	LW5	8.08	88.36	11.64	1.878	20.54	32.17
	LW6	8.33	91.10	8.90	0.61	6.67	15.57
	LW7	7.41	81.04	18.96	5.133	56.14	75.10
	LW8	7.15	78.19	21.81	5.143	56.24	78.05
2	LW9	6.9	75.46	24.54	4.723	51.65	76.19
	LW10	6.64	72.62	27.38	4.713	51.54	78.93
	LW11	6.39	69.88	30.12	4.633	50.67	80.79
	LW12	6.13	67.04	32.96	2.833	30.98	63.94
	LW13	6.93	75.79	24.21	3.05	33.36	57.57
	LW14	6.87	75.13	24.87	3.36	36.75	61.61
3	LW15	6.81	74.48	25.52	3.15	34.45	59.97
	LW16	6.74	73.71	26.29	3.01	32.92	59.21
	LW17	6.68	73.05	26.95	2.96	32.37	59.32
	LW18	6.61	72.29	27.71	3.72	40.68	68.39
	LW19	9.144	100.00	0.00	6.774	74.08	74.08
	LW20	9.144	100.00	0.00	5.081	55.57	55.57
4	LW21	9.144	100.00	0.00	5.356	58.57	58.57
	LW22	9.144	100.00	0.00	5.706	62.40	62.40
	LW23	9.144	100.00	0.00	5.846	63.93	63.93
	LW24	9.144	100.00	0.00	6.286	68.74	68.74
	LW25	6.4	69.99	30.01	3.24	35.43	65.44
	LW26	6.52	71.30	28.70	3.55	38.82	67.52
5	LW27	6.03	65.94	34.06	3.96	43.31	77.36
	LW28	6.11	66.82	33.18	4.11	44.95	78.13
	LW29	6.51	71.19	28.81	4.28	46.81	75.61
	LW30	6.43	70.32	29.68	3	32.81	62.49

Trial conducted at 10.3 km h^{-1} [6.4 mph]. Target area 9.14 m^2. Size identifier LW.

Table A5. Second and final trial raw cell length testing results for 1.52 m.

Cell ID	Speed (mph)	Spray Cvg. Area	% Sprayed	% Underspray	Overspray Cvg. Area	% Overspray	% Difference
LS1	6.4	11.43	100.00	0.00	5.54	48.47	48.47
LS2	6.4	11.19	97.90	2.10	12.762	111.65	113.75
LS3	6.4	5.41	47.33	52.67	4.87	42.61	95.28
LS4	6.4	4.76	41.64	58.36	4.78	41.82	100.17
LS5	6.4	3.8	33.25	66.75	4.14	36.22	102.97
LS6	8.4	6.03	52.76	47.24	6.38	55.82	103.06
LS7	8.4	1.06	9.27	90.73	12.04	105.34	196.06
LS8	8.4	3.17	27.73	72.27	7.42	64.92	137.18
LS9	8.4	3.46	30.27	69.73	7.02	61.42	131.15
LS10	8.4	3.62	31.67	68.33	7.04	61.59	129.92
LS11	4.4	8.69	76.03	23.97	9.22	80.66	104.64
LS12	4.4	11.43	100.00	0.00	12.762	111.65	111.65
LS13	4.4	11.43	100.00	0.00	12.762	111.65	111.65
LS14	4.4	10.87	95.10	4.90	4.99	43.66	48.56
LS15	4.4	6.67	58.36	41.64	7.61	66.58	108.22

Target area 11.43 m^2. Size identifier LS.

Table A6. Second and final trial raw cell length testing results for 3.05 m.

Cell ID	Speed (mph)	Spray Cvg. Area	% Sprayed	% Underspray	Overspray Cvg. Area	% Overspray	% Difference
LM1	6.4	22.86	100.00	0.00	7.31	31.98	31.98
LM2	6.4	22.86	100.00	0.00	10.89	47.64	47.64
LM3	6.4	17.28	75.59	24.41	5.8	25.37	49.78
LM4	6.4	15.62	68.33	31.67	10.48	45.84	77.52
LM5	6.4	15.86	69.38	30.62	7.61	33.29	63.91
LM6	8.4	19.4	84.86	15.14	6.13	26.82	41.95
LM7	8.4	12.86	56.26	43.74	5.05	22.09	65.84
LM8	8.4	17.51	76.60	23.40	8.31	36.35	59.76
LM9	8.4	13.89	60.76	39.24	2.76	12.07	51.31
LM10	8.4	17.04	74.54	25.46	13.524	59.16	84.62
LM11	4.4	20.75	90.77	9.23	11.6	50.74	59.97
LM12	4.4	22.86	100.00	0.00	13.524	59.16	59.16
LM13	4.4	22.86	100.00	0.00	13.524	59.16	59.16
LM14	4.4	22.86	100.00	0.00	13.524	59.16	59.16
LM15	4.4	18.29	80.01	19.99	13.524	59.16	79.15

Target area 22.86 m^2. Size identifier LM.

Table A7. Second and final trial raw cell length testing results for 4.57 m.

Cell ID	Speed (mph)	Spray Cvg. Area	% Sprayed	% Underspray	Overspray Cvg. Area	% Overspray	% Difference
LL1	6.4	33.92	98.92	1.08	7.24	21.11	22.19
LL2	6.4	31.16	90.87	9.13	7.8	22.75	31.88
LL3	6.4	28.93	84.37	15.63	8.61	25.11	40.74
LL4	6.4	28.8	83.99	16.01	6.28	18.31	34.32
LL5	6.4	28.92	84.34	15.66	14.286	41.66	57.32
LL6	8.4	32.77	95.57	4.43	9.09	26.51	30.94
LL7	8.4	24.97	72.82	27.18	7.98	23.27	50.45
LL8	8.4	31.23	91.08	8.92	5.55	16.19	25.11
LL9	8.4	25.32	73.84	26.16	2.09	6.10	32.25
LL10	8.4	22.55	65.76	34.24	9.25	26.98	61.21
LL11	4.4	32.82	95.71	4.29	8.27	24.12	28.40
LL12	4.4	34.29	100.00	0.00	14.286	41.66	41.66
LL13	4.4	34.29	100.00	0.00	14.286	41.66	41.66
LL14	4.4	31.59	92.13	7.87	12.97	37.82	45.70
LL15	4.4	29.18	85.10	14.90	14.286	41.66	56.56

Target area 34.29 m^2. Size identifier LL.

Table A8. Second and final trial raw cell length testing results for 6.10 m.

Cell ID	Speed (mph)	Spray Cvg. Area	% Sprayed	% Underspray	Overspray Cvg. Area	% Overspray	% Difference
LX1	6.4	44.46	97.24	2.76	5.43	11.88	14.63
LX2	6.4	40.11	87.73	12.27	8.3	18.15	30.42
LX3	6.4	39.94	87.36	12.64	5.32	11.64	24.28
LX4	6.4	39.66	86.75	13.25	3.76	8.22	21.48
LX5	6.4	38.63	84.49	15.51	3.31	7.24	22.75
LX6	8.4	45.63	99.80	0.20	9.09	19.88	20.08
LX7	8.4	37.04	81.01	18.99	4.03	8.81	27.80
LX8	8.4	28.04	61.33	38.67	2.34	5.12	43.79
LX9	8.4	35.26	77.12	22.88	2.92	6.39	29.27
LX10	8.4	35.58	77.82	22.18	3.2	7.00	29.18
LX11	4.4	45.28	99.04	0.96	15.048	32.91	33.88
LX12	4.4	45.72	100.00	0.00	15.048	32.91	32.91
LX13	4.4	45.72	100.00	0.00	12.6	27.56	27.56
LX14	4.4	43.15	94.38	5.62	7.57	16.56	22.18
LX15	4.4	40.8	89.24	10.76	10.72	23.45	34.21

Target area 45.72 m^2. Size identifier LX.

Table A9. Summary of the evaluation of field spraying accuracy using a Case IH Patriot 4440 and a prescription map with variable cell width (SW=0.5 m, MW=1.5 m, and LW=3 m) as input. Cell length were kept constant (3.1 m) and the application speed was set to 10.3 km h^{-1}.

Cell Size ID	Target Area (m^2)	Actual Coverage (m^2)	Overspray Coverage (m^2)	Undersprayed % Area	Oversprayed % Area
SW	1.524	1.52	1.84	0.37	120.95
SW	1.524	1.20	1.74	21.04	114.06
SW	1.524	1.01	1.49	33.84	97.88
SW	1.524	1.52	2.81	0.00	184.20
SW	1.524	1.41	2.52	7.48	165.35
MW	4.572	4.34	1.65	5.18	36.02
MW	4.572	4.00	1.81	12.44	39.59
MW	4.572	3.23	2.75	29.32	60.13
MW	4.572	4.38	3.42	4.20	74.84
MW	4.572	3.69	3.22	19.29	70.32
LW	9.144	8.13	2.03	11.13	22.21
LW	9.144	6.77	4.53	25.96	49.54
LW	9.144	6.77	3.21	25.93	35.09
LW	9.144	9.14	5.84	0.00	63.88
LW	9.144	6.33	3.69	30.74	40.35
---------- Treatment Means ----------					
SW	1.524	1.33	2.08	12.55	136.49
MW	4.572	3.93	2.57	14.09	56.18
LW	9.144	7.43	3.86	18.75	42.22

Each treatment replicate is composed of six measurements across the sprayer boom. The treatment means for each cell size are composed of 30 measurements.

Figure A1. Case Patriot 4440 self-propelled sprayer. Photographed at CREC.

Figure A2. Case Patriot 4440 self-propelled sprayer applicating red dye solution during the initial trial. Photographed at CREC.

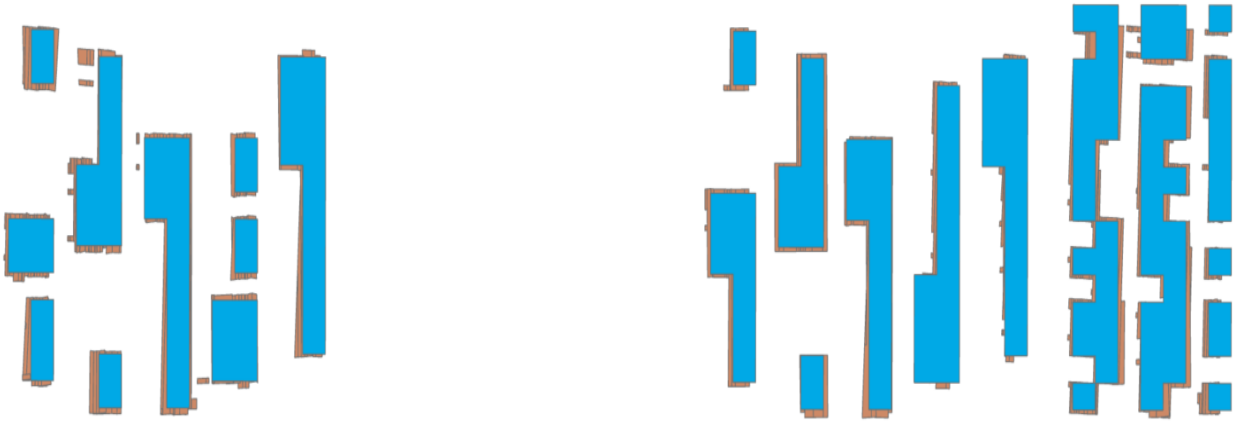

Figure A3. First field trial as-applied map overlayed with software modified prescription map. Brown is as-applied polygons denoting applicated rate of 15 gal/ac, blue is prescription map.

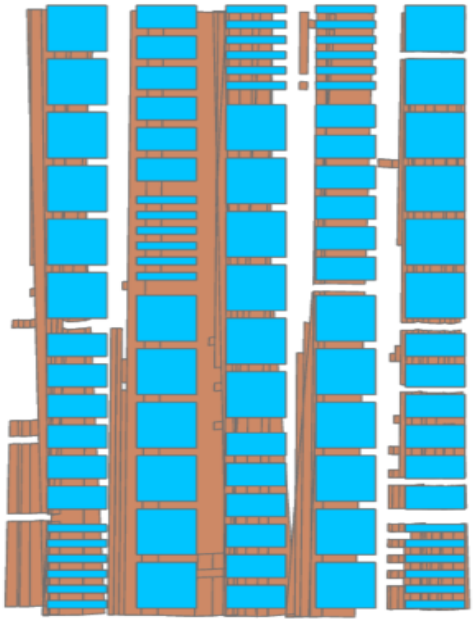

Figure A4. Final field trial cell width study as-applied map overlayed with prescription map. Brown is as-applied polygons denoting applicated rate of 15 gal/ac, blue is prescription map.

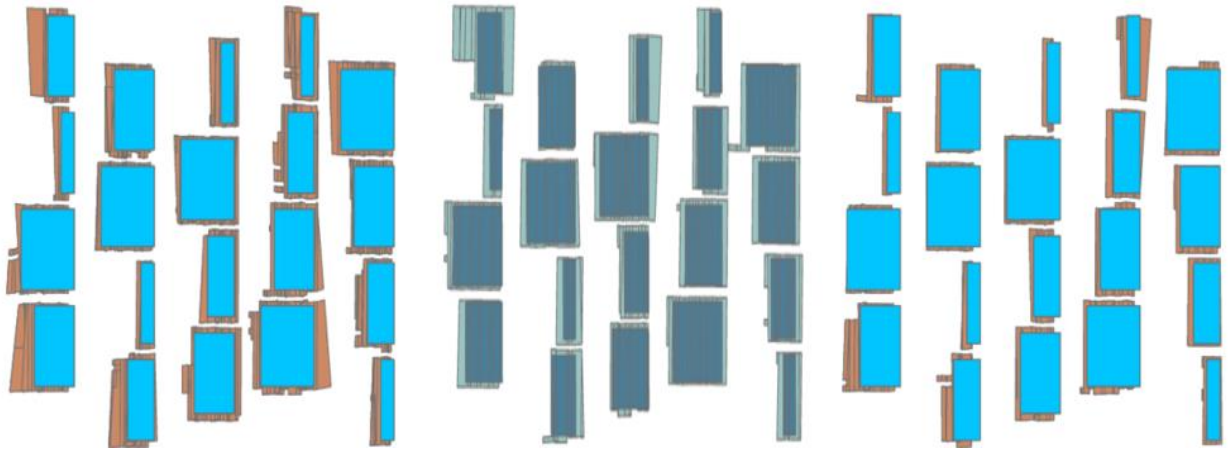

Figure A5. Final field trial speed study combining pass 1 (light blue) and pass 2 (dark blue) as-applied map overlayed with prescription map. Brown and light green is as-applied polygons denoting applicated rate 15 gal/ac, blue and dark blue is prescription map.

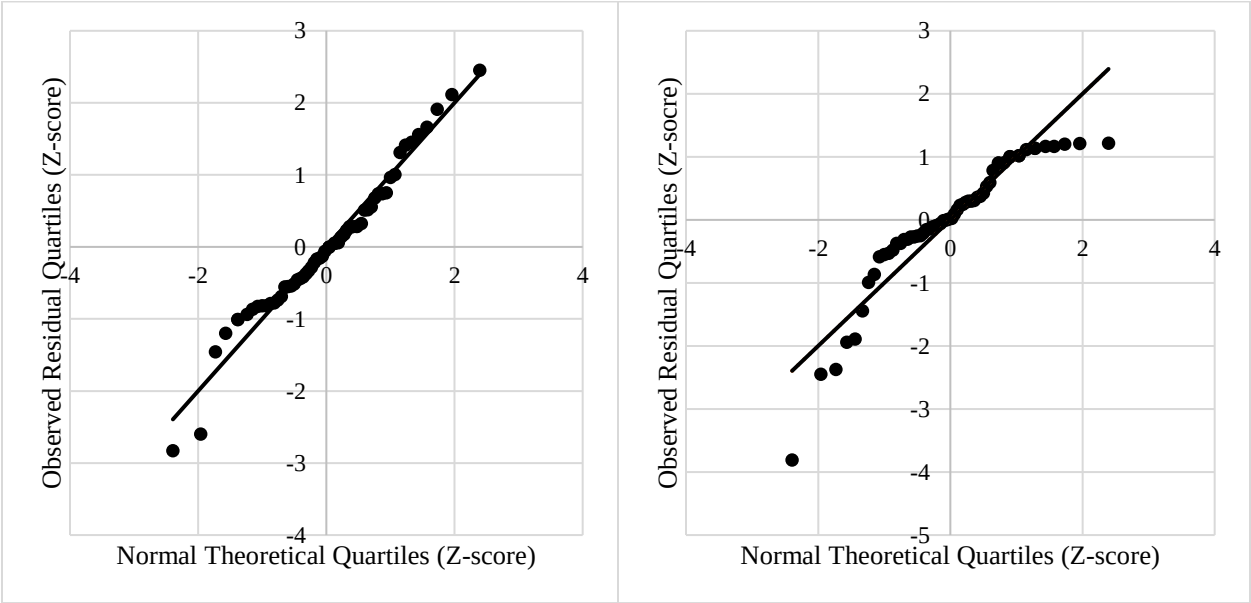

Figure A6. Q-Q plots of model residuals for percent area underspray, assuming a gaussian distribution with identity linkage (Left) and assuming a beta distribution with logit linkage (Right).

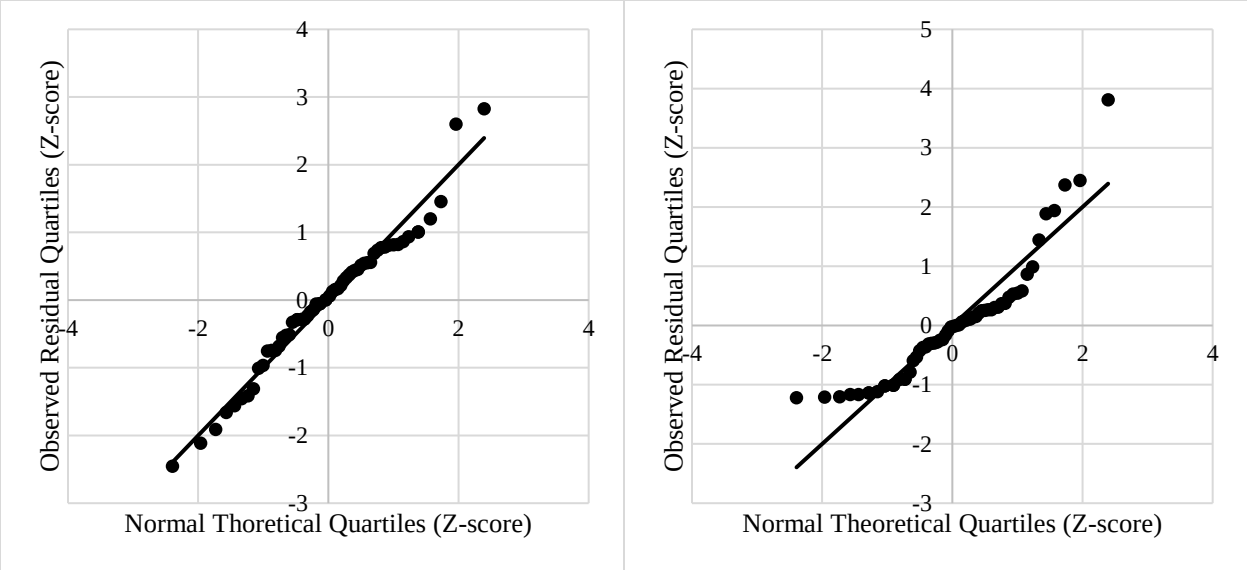

Figure A7. Q-Q plots of model residuals for percent area overspray, assuming a gaussian distribution with identity linkage (Left) and assuming a beta distribution with logit linkage (Right).